CHAPTER IV

RESULTS AND DISCUSSION

4.1 The physico-chemical properties of MCM-22

4.1.1 XRD results

The XRD patterns of as-synthesized MCM-22 and calcined MCM-22 zeolite samples with the SiO_2/Al_2O_3 ratio in gel composition of 30 are shown in Figure 4.1. XRD pattern of the as-synthesized MCM-22 in Figure 4.1 (a) exhibits the peak positions located at $2\Theta = 3.22^{\circ}$, 6.72° and 7.14° which are indexed as [001], [002] and [100], respectively. This refers to the lamella structure of MCM-22 precursor [40, 41]. In Figure 4.1(b), both [001] and [002] peaks disappear but the intensity of [100] peak at $2\Theta \approx 7^{\circ}$ becomes stronger than the as-synthesized sample due to the formation of three-dimensional MCM-22 structure after calcination.

The sample of MCM-22 was synthesized by one step of crystallization and crystallization time was varied. The formation of MCM-22 is initiated between 3.5 and 4 days [Figure 4.2(b) and 4.2(c)] but is not yet complete. Increasing crystallization time from 3.5 to 7 days results in the increase in crystallinity of the samples [Figure 4.2(b)-(e)]. The crystallinity does not increase further after 7.5 days but produces the impurity phase that appears at $2\theta \approx 9^{\circ}$ in the XRD pattern [Figure 4.2(f)]. Therefore, the crystallization at 140°C for 7 days is utilized.

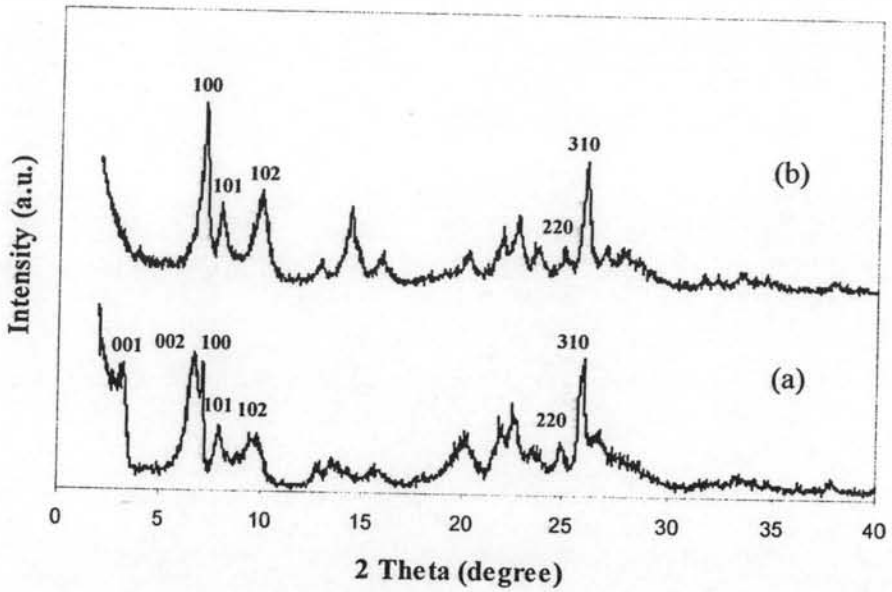

Figure 4.1 XRD patterns of (a) as-synthesized and (b) calcined MCM-22 zeolite (SiO_2/Al_2O_3 in gel = 30).

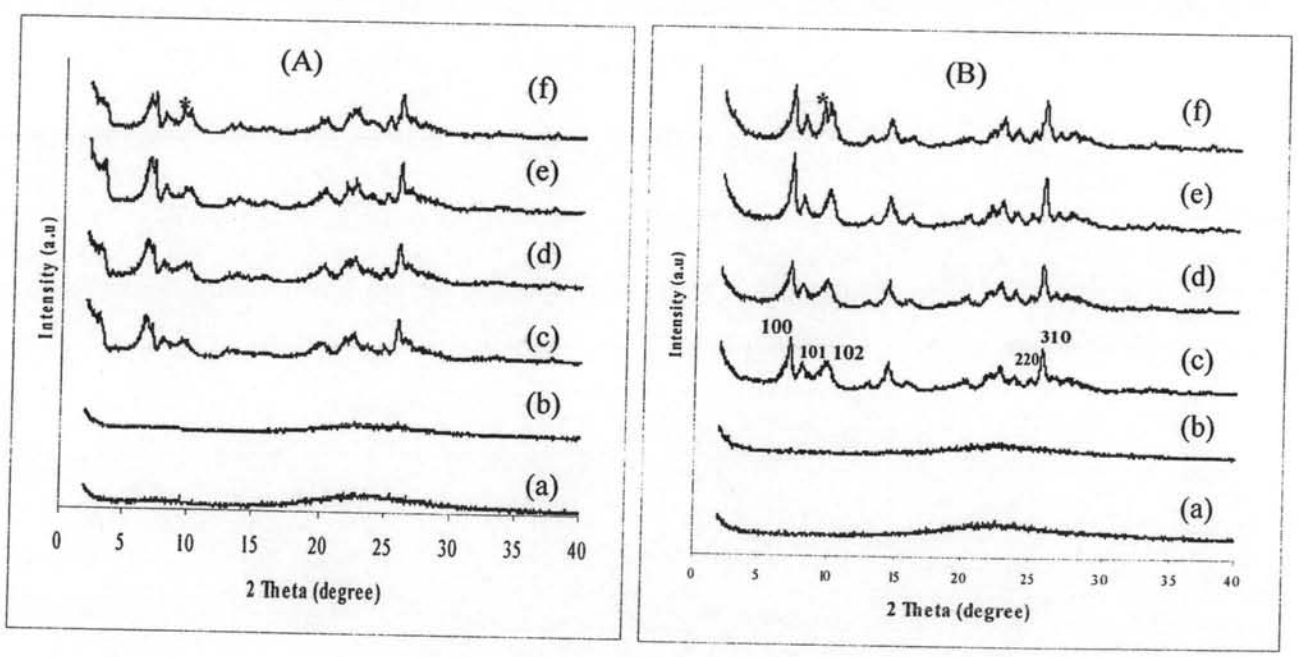

Figure 4.2 XRD patterns of as-synthesized (A) and calcined MCM-22 zeolite (B) with different crystallization time, (a) 3 days, (b) 3.5 days, (c) 4 days, (d) 5 days, (e) 7 days and (f) 7.5 days.

The synthesized MCM-22 material is treated with 1 M NH_4Cl solution for 2 h, 5 times; this is denoted as H-MCM-22 catalyst. The XRD patterns of calcined H-MCM-22 zeolite with different SiO_2/Al_2O_3 ratios in gel are presented in Figure 4.3. Distinct patterns are observed for H-MCM-22(30) and H-MCM-22(60), and 2θ value of patterns are comparable to the previous literature [40]. The XRD pattern of H-MCM-22(120) reveals the slight decrease of the crystallinity. For H-MCM-22(400) shows obviously decreasing in the crystallinity. Hence, gel composition with SiO_2/Al_2O_3 of 400 might not be suitable for synthesis H-MCM-22. This study suggests that the workable range of SiO_2/Al_2O_3 ratio for good synthesis of H-MCM-22 is between 30 to 250.

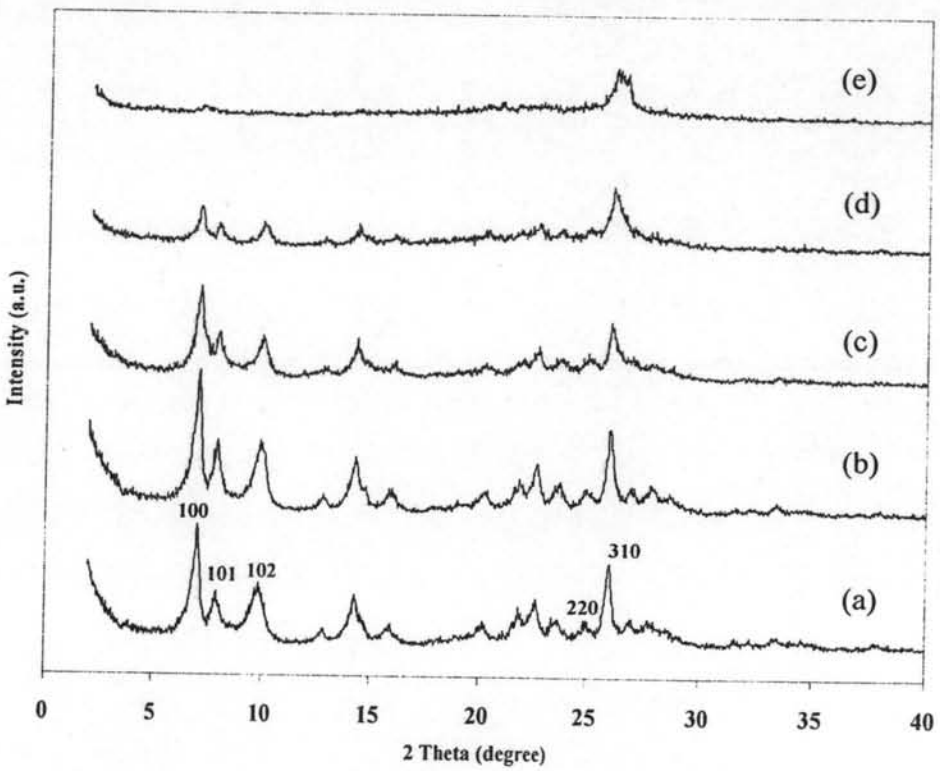

Figure 4.3 XRD patterns of calcined MCM-22 with different SiO_2/Al_2O_3 ratios, (a) $SiO_2/Al_2O_3 = 30$, (b) $SiO_2/Al_2O_3 = 60$, (c) $SiO_2/Al_2O_3 = 120$, (d) $SiO_2/Al_2O_3 = 250$ and (e) $SiO_2/Al_2O_3 = 400$.

4.1.2 Elemental analysis

The SiO_2/Al_2O_3 ratios in gel composition and in H-MCM-22 materials are compared in Table 4.1. The SiO_2/Al_2O_3 ratios in catalyst and gel composition are different in which catalyst is half of gel composition from sample with SiO_2/Al_2O_3 ratio 60 up. The elemental analysis result suggests that the parts of aluminum are in the structure of catalyst. However, data from only ICP-AES technique cannot exhibit the position of aluminum atom, whether it located in framework or extra-framework, therefore data from ^{27}Al-NMR is need for identification.

Table 4.1 SiO_2/Al_2O_3 ratios in gel composition and in product of H-MCM-22 catalysts.

Sample	SiO_2/Al_2O_3 ratio	
	in gel composition [a]	in catalysts [b]
H-MCM-22 (30)	30	24.68
H-MCM-22 (60)	60	38.08
H-MCM-22 (120)	120	83.26
H-MCM-22 (250)	250	165.26
H-MCM-22 (400)	400	199.60

a: Calculated from reagent quantities
b: Aluminum (Al) was determined by ICP-AES and Na was determined by AAS.

4.1.3 SEM images of MCM-22

The SEM images of Na-MCM-22 and H-MCM-22 samples are shown in Figure 4.4. Comparing SEM pictures, the size of MCM-22 particles is unchanged after NH_4Cl treatment. All calcined samples are aggregates of platelets with irregular shape. The average size of particles is 0.8 μm in length and 0.4 μm in thickness. The platelets are not seen to possess well-defined morphology.

Figure 4.4 SEM images of calcined sample (A) Na-MCM-22(30), (B) H-MCM-22(30), (c) H-MCM-22(60) and (d) H-MCM-22(120) catalysts.

4.1.4 ^{27}Al-MAS-NMR spectra

Solid state ^{27}Al-MAS-NMR can provide the information of the aluminum atom that located at the framework or non-framework site. In Figure 4.5 and Figure 4.6 show ^{27}Al-MAS-NMR spectra of MCM-22 catalysts, the signal at 50 ppm is typically assigned to tetrahedrally coordination (T_d) framework aluminum, and the peak at 0 ppm is assigned to the octahedrally coordination (O_h) non-framework aluminum [69]. The two signals of aluminum atoms at framework sites are observed for Na-MCM-22 sample Figure 4.5 (a) which the relative amounts of the tetrahedral (T) and octahedral (O) aluminum atoms are I_T/I_O = 1: 0.23. However, it cannot tell whether the counter ions are totally H^+ or Na^+. It is necessary to change sodium ions in catalysts to protons form in order to enhance the acid properties of MCM-22 as described in section 3.6. The ^{27}Al-MAS-NMR spectra of H-MCM-22 sample after NH_4Cl treatment are presented in Figure 4.5 (b). It is observed that the signal at 0 ppm shows slightly lower

intensity than Na-MCM-22 sample and the I_T/I_O is 1: 0.18. This result indicates that aluminum at octahedral sites decrease after NH_4Cl treatment.

The ^{27}Al-MAS-NMR spectra of MCM-22 catalysts with various SiO_2/Al_2O_3 ratios after treated with 1 M NH_4Cl solution are presented in Figure 4.6. As SiO_2/Al_2O_3 ratios increase, aluminum content decrease, the signals at both sites decrease in intensity. However, the aluminum atoms preferably remain at tetrahedral framework position.

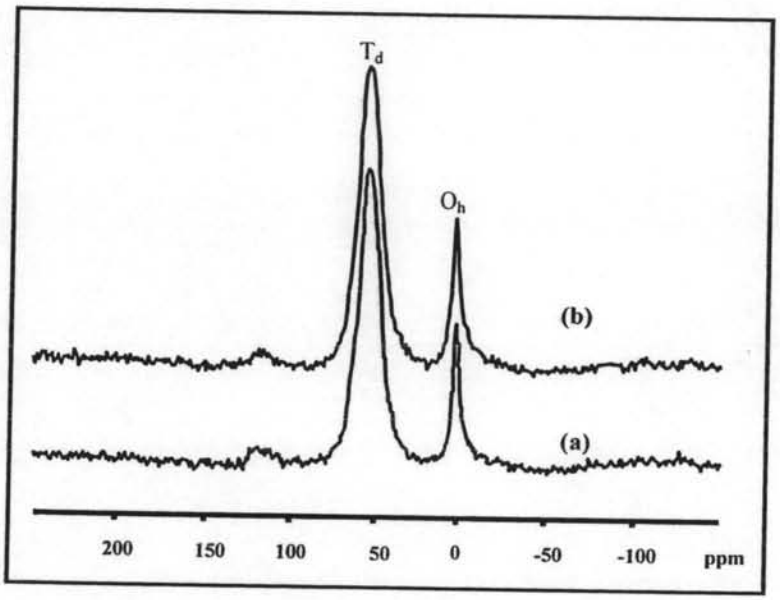

Figure 4.5 The ^{27}Al-MAS-NMR Spectra of (a) Na-MCM-22(30) and (b) H-MCM-22(30) catalysts.

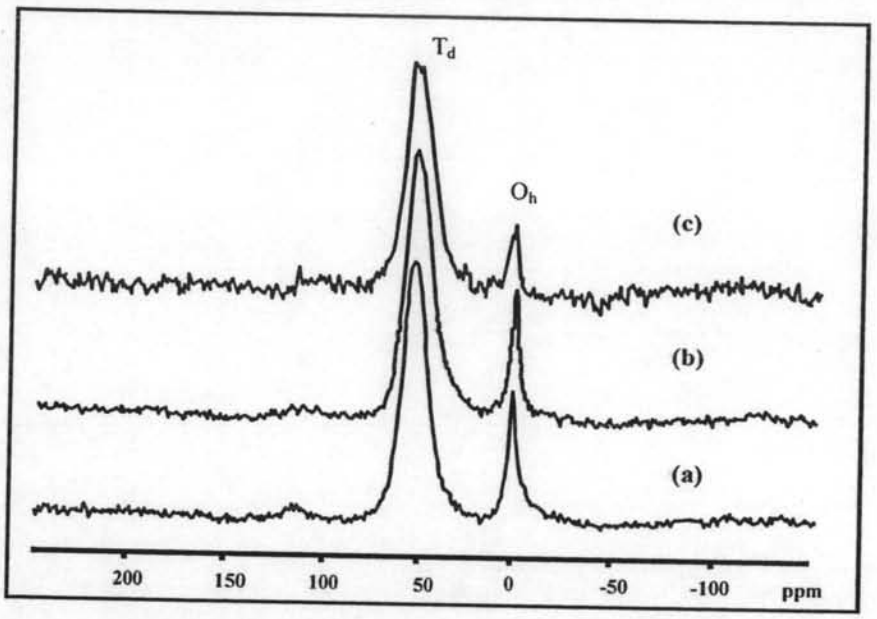

Figure 4.6 The ^{27}Al-MAS-NMR Spectra of (a) H-MCM-22(30), H-MCM-22(60), and (c) H-MCM-22(120) catalysts.

4.1.5 Acidity of MCM-22 catalysts

Figure 4.7 shows NH_3-TPD profiles of H-MCM-22 catalysts with different SiO_2/Al_2O_3 ratios. The peak contented lower than 200°C is typically assigned to a weaker acid sites, another small peak at 350°C is assigned to a strong acid site. The acid strength is similar for all catalysts, and only the numbers of acid sites are different between Na-form and H-form which Na-form contains less acid site than H-form in Figure 4.7(A). When SiO_2/Al_2O_3 ratio is increase from 30 to 400 in Figure 4.8(B); the signals at both sites decrease, respectively due to decreasing of aluminum content in samples. The NH_3-TPD profiles indicate that almost catalysts exhibit two NH_3 desorption peaks except for a low aluminum content, sample H-MCM-22(400), shows only one desorption peak, at 170°C. The number of strong acid sites is pronounced for H-MCM-22(30) and decrease from H-MCM-22(60) to H-MCM-22(400), respectively.

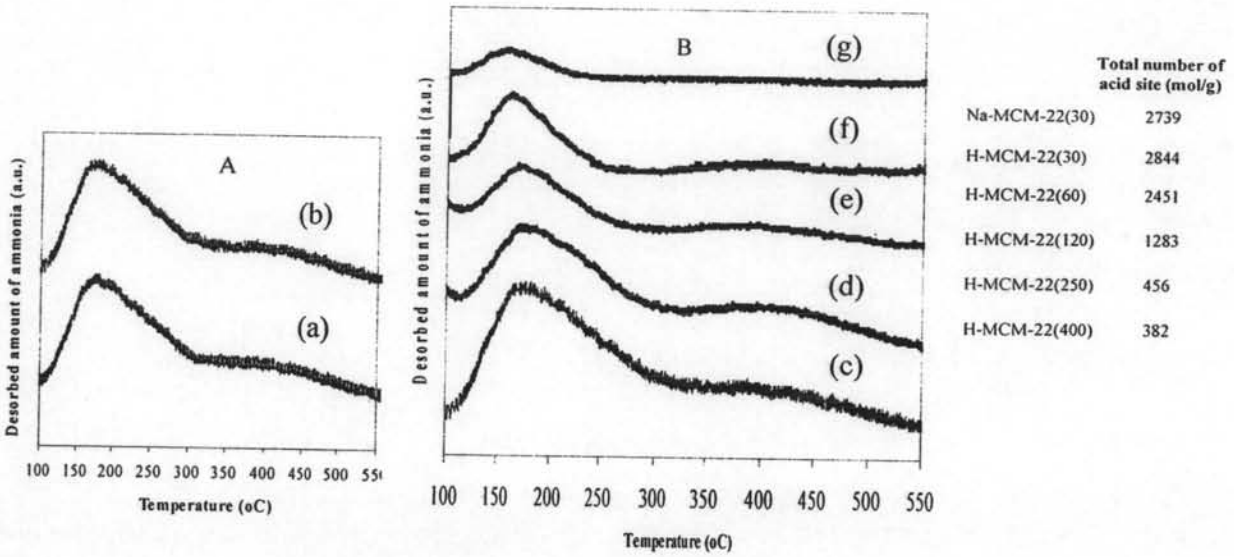

Figure 4.7 NH_3-TPD profiles of samples (a) Na-form, (b) H-form, (c) H-MCM-22(30), (d) H-MCM-22(60), (e) H-MCM-22(120), (f) H-MCM-22(250) and (g) H-MCM-22(400).

4.1.6 Sorption properties of MCM-22

The N_2 adsorption-desorption isotherms of the calcined H-MCM-22 catalysts with various SiO_2/Al_2O_3 ratios are shown in Figure 4.8. All samples exhibit type I isotherm which is typical for microporous material. Textural properties of calcined H-MCM-22 catalysts are shown in Table 4.2. Increasing the SiO_2/Al_2O_3 ratio from 60 to 400 leads to a reduction in the amount of nitrogen up taken due to the decrease of micropore volume. H-MCM-22(60) provides highest specific surface area. The pore size distribution number, obtained from adsorption data, is 0.6 for all H-MCM-22 catalysts.

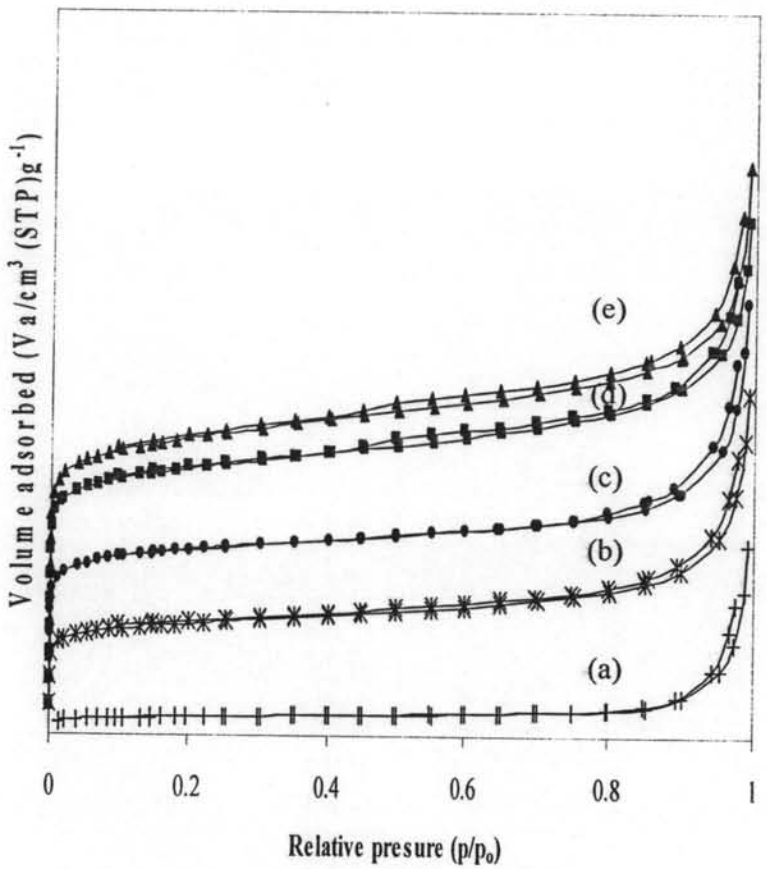

Figure 4.8 N_2 adsorption-desorption isotherm of (a) H-MCM-22(400), (b) H-MCM-22(250), (c) H-MCM-22(120), (d) H-MCM-22(30) and (e) H-MCM-22(60).

Table 4.2 Textural properties of calcined H-MCM-22 catalysts

Sample	Total specific sureface area[a] (m^2/g)	External surface area[b] (m^2/g)	Micropore distribution[c] (nm.)	Micropore volume[b] (cm^3/g)
H-MCM-22 (30)	487	60	0.60	0.18
H-MCM-22 (60)	540	56	0.60	0.21
H-MCM-22 (120)	362	41	0.60	0.14
H-MCM-22 (250)	202	42	0.60	0.07
H-MCM-22 (400)	32	12	0.60	0.01

[a] *Calculated using the BET plot method,*

[b] *Calculated using the t- plot method,*

[c] *Calculated using the MP- plot method*

4.2 Activity of various catalytic in PP waste cracking

4.2.1 Effect of sodium ion in catalyst

The values of % conversion and product yield obtained by the catalytic cracking of PP waste over Na-MCM-22, H-MCM-22 and thermal cracking at 380°C are compared in Table 4.3. Almost H-MCM-22 catalysts show higher conversion than Na-MCM-22, except H-MCM-22(30) and Na-MCM-22(30) are not significantly different. Considering product yield, catalytic cracking of PP waste over all MCM-22 catalysts produced higher gas fraction than liquid fraction which give the same result when using ZSM-5 as catalyst [70]. The yields of gas fraction are in the range of 32-54% while that of liquid fraction is about 24-38%. With higher SiO_2/Al_2O_3 ratios above 30 the catalysts perform higher % conversion after they are changed to proton form. This effect is from the removal of trace amount of Na^+ ion by NH_4Cl treatment. For the catalyst with SiO_2/Al_2O_3 of 30, relatively high aluminum content, there are no differences in % conversion between the activity of H-MCM-22 and Na-MCM-22 catalysts due to large amount of acid site in MCM-22(30) samples. The H-MCM-22(120) catalyst exhibits the highest conversion about 92%, 54% yield of gas fraction, 38% yield of liquid fraction and small amount of residue. This result can be explained by lower aluminum at octahedral sites in H-MCM-22(120) than H-MCM-22(30).

The result also indicates that MCM-22 can perform as catalyst in cracking of PP waste at high conversion. Treatment of MCM-22 with 1.0 M NH_4Cl solution promotes the conversion in case of mild or low acidity, but high aluminum content or high acidity catalyst does not show significant difference. However, the presence of Na^+ even in a small amount in catalyst makes a decrease in activity of the acid catalyst in PP waste cracking. H-MCM-22 catalysts provide more light oil than heavy oil. The color of liquid fraction of H-MCM-22 catalyst is lighter than those Na-MCM-22 catalysts.

Selectivity to liquid fraction is increased in the order of H-MCM-22(120) ≈ H-MCM-22(250) ≈ Na-MCM-22(120) > Na-MCM-22(30) ≈ H-MCM-22(30) > Na-MCM-22(250) while the heavy oil is in the opposite order. Nevertheless, all MCM-22 catalysts have much greater total volume of liquid fraction than thermal cracking. Residue, referred to all remaining in the reactor except catalyst, is identified as solid coke deposit on catalyst and wax. At higher conversion, residue in term of wax decease.

Table 4.3 Conversion and product yield from PP waste cracking over H-MCM-22 with various SiO_2/Al_2O_3 ratios (Condition: 10%wt catalyst of PP waste, N_2 flow of 20 cm^3/min, 380°C and reaction time of 40 min)

	SiO_2/Al_2O_3 ratios in catalyst						Thermal cracking
	Na-MCM-22 (30)	H-MCM-22 (30)	Na-MCM-22 (120)	H-MCM-22 (120)	Na-MCM-22 (250)	HMCM-22 (250)	
Conversion[a] (%)	82.40	81.50	86.10	91.60	56.90	83.87	23.60
Yield[b] (%)							
1. gas fraction	51.40	52.20	49.60	53.60	32.90	46.60	12.20
2. liquid fraction	31.00	29.30	36.50	38.00	24.00	37.27	11.40
- % distillated oil	55.15	64.97	51.68	57.99	51.08	52.34	54.87
- % heavy oil	44.85	35.03	48.33	42.01	48.93	47.66	45.13
3. residue	17.60	18.50	13.90	8.40	43.10	16.13	76.40
- wax	5.86	5.48	6.04	5.05	7.65	7.50	-
- solid coke	11.74	13.02	7.86	3.36	35.45	8.63	-
Total volume of liquid fraction (cm^3)	2.05	2.00	2.50	2.63	1.70	2.55	0.45
Liquid fraction density (g/cm^3)	0.75	0.74	0.73	0.73	0.71	0.73	0.72

[a] *Deviation within 0.40 %*

[b] *Deviation within 0.50 %*

Figure 4.9 shows the volume of accumulative volume of liquid fraction in the graduated cylinder obtained by catalytic cracking of PP waste over various Na-MCM-22 and H-MCM-22 catalysts at 380°C. This plot accounts for the kinetic rate of this reaction. For thermal cracking, the least liquid is found in the graduated cylinder. The kinetic rate in liquid fraction is very slow with the final accumulative volume of liquid only 0.45 cm^3. From the data obtained, it is found that H-MCM-22(250) catalyst shows rate of liquid fraction formation faster than Na-MCM-22(250) catalyst, while other catalysts are no significant difference in kinetic rate between treated catalyst and untreated catalyst. The effect of NH_4Cl treatment is more pronounced for the catalyst with SiO_2/Al_2O_3 ratio of 250 due to containing small amount of acid sites. However, it can be concluded that a small amount of Na^+ in low Al content catalyst still affects the

rate of reaction thus NH_4Cl treatment is a necessary required to modify MCM-22 catalyst.

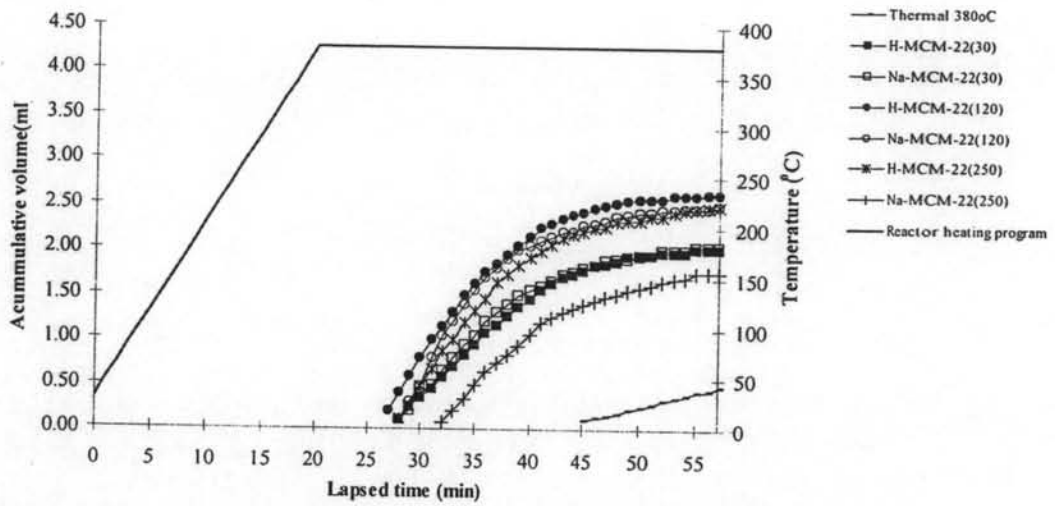

Figure 4.9 Accumulative volume of liquid fractions from catalytic cracking of PP waste over Na-MCM-22 and H-MCM-22 at 380°C (Condition: 10%wt catalyst of PP waste, N_2 flow of 20 cm^3/min and reaction time of 40 min).

Figure 4.10 shows distribution of gas fraction obtained by catalytic cracking of PP waste over various MCM-22 catalysts at 380°C. In the presence of MCM-22 catalysts, the product distribution in gas fraction is much different from thermal cracking. Significant product selectivity to propene and n-pentane are found for thermal cracking while, MCM-22(30) catalytic cracking promotes n-butane as a major gas product. Other MCM-22 catalysts provide C_5^+, propene and n-butane as main three gas products.

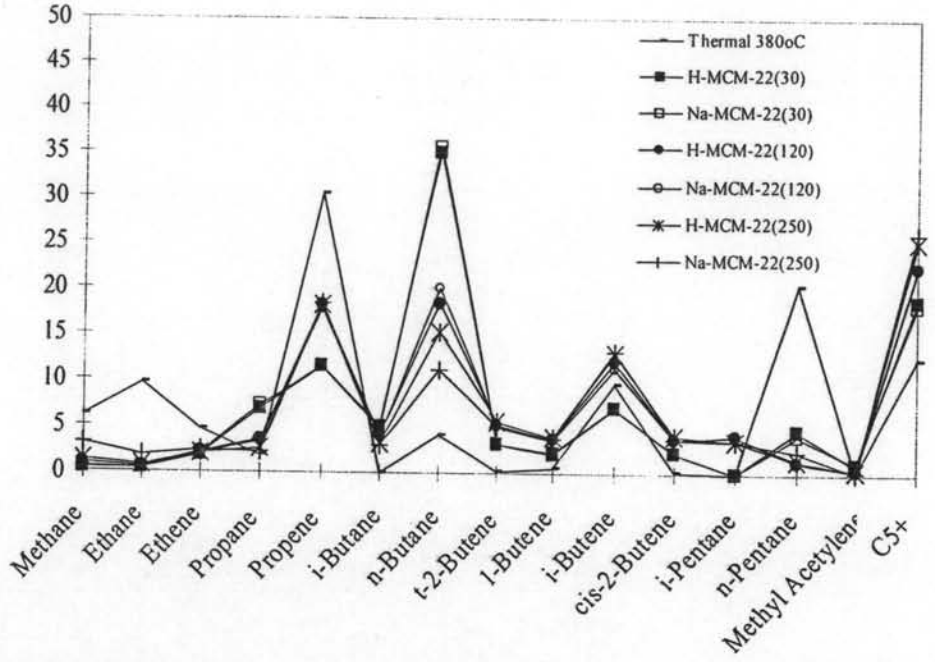

Figure 4.10 Distribution of gas fraction obtained by catalytic cracking of PP waste over Na-MCM-22 and H-MCM-22 at 380°C (Condition: 10%wt catalyst of PP waste, N_2 flow of 20 cm^3/min and reaction time of 40 min).

Figure 4.11 shows production distribution of distillated oil fraction obtained by catalytic cracking of PP waste over various MCM-22 catalysts at 380°C. Liquid product is identified with the C_{np} value which related to the boiling of normal paraffins [73]. For thermal cracking promotes the liquid product mainly in the range of C_8 – C_{10} hydrocarbons with C_9 as the predominate product which different from the reaction in the presence of MCM-22 catalysts. The product distributions in liquid phase are the same trend for sample Na-MCM-22 and H-MCM-22 which promote C_7-C_8 hydrocarbons at the same composition range to gasoline.

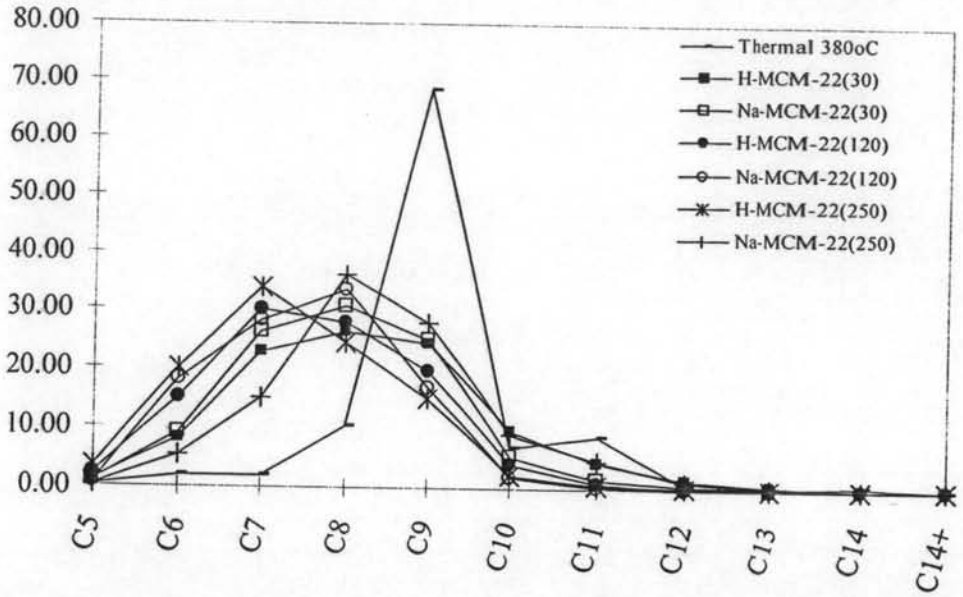

Figure 4.11 Carbon number distribution of distillated oil obtained by catalytic cracking of PP waste over Na-MCM-22 and H-MCM-22 at 380°C (Condition: 10%wt catalyst of PP waste, N_2 flow of 20 cm^3/min and reaction time of 40 min).

4.2.2 Effect of aluminum content in catalyst

The value of % conversion and product yield obtained by PP waste cracking over H-MCM-22 with different SiO_2/Al_2O_3 ratios at 380°C are compared in Table 4.4. Considering data, the increase SiO_2/Al_2O_3 ratios from 30 to 120 lead to increase 10% conversion from 82% to 92%. When SiO_2/Al_2O_3 ratio increases to 250 and 400, the conversion reduce to 84% and 76%, respectively. Therefore, H-MCM-22(60) and H-MCM-22(120) provide the highest conversion. For less conversion of H-MCM-22(30) catalyst causes lower total surface area than H-MCM-22(60) while that of H-MCM-22(250) and H-MCM-22(400) depend on both low surface area and acidity.

The H-MCM-22(60) showed the highest gas fraction due to its high specific surface area. For H-MCM-22(120), the yield of gas fraction decreases while liquid fraction increases due to the decreasing of acidity to promote over cracking to gas product. The high total surface area of MCM-22 catalyst makes rise in conversion of PP waste and remains low residue. When SiO_2/Al_2O_3 ratio increases from 30 to 400, the

selectivity to light oil fraction decreases while heavy oil increases according to the acidity of catalyst.

Table 4.4 Conversion and product yield from PP waste cracking over H-MCM-22 with various SiO_2/Al_2O_3 ratios (Condition: 10%wt catalyst of PP waste, N_2 flow of 20 cm^3/min, 380°C and reaction time of 40 min)

	SiO_2/Al_2O_3 ratios in catalyst				
	30	60	120	250	400
Conversion[a] (%)	81.50	92.47	91.60	83.87	76.10
Yield[b] (%)					
1. gas fraction	52.20	57.07	53.60	46.60	41.30
2. liquid fraction	29.30	35.40	38.00	37.27	34.80
- % distillated oil	64.97	63.80	57.99	52.34	51.82
-% heavy oil	35.03	36.20	42.01	47.66	48.18
3. residue	18.50	7.53	8.40	16.13	23.90
- wax	13.02	4.92	5.05	7.50	9.10
- solid coke	5.48	2.61	3.36	8.63	14.81
Total volume of liquid fraction (cm^3)	1.98	2.40	2.63	2.55	2.48
Liquid fraction density (g/cm^3)	0.74	0.74	0.73	0.73	0.72

[a] *Deviation within 0.60 %*

[b] *Deviation within 0.50 %*

Figure 4.12 shows the accumulated volume of liquid fraction obtained by catalytic cracking of PP waste over H-MCM-22 catalyst with various SiO_2/Al_2O_3 ratios at 380°C along the formation of liquid for H-MCM-22(60) and H-MCM-22(120) are not different. But the rate over H-MCM-22(60) is faster than over H-MCM-22(120) in the initial step. This is the effect of acidity of catalyst or SiO_2/Al_2O_3 ratios of 60 and 400 are obviously slower than other catalysts. Therefore, the total liquid volumes of these catalysts are different.

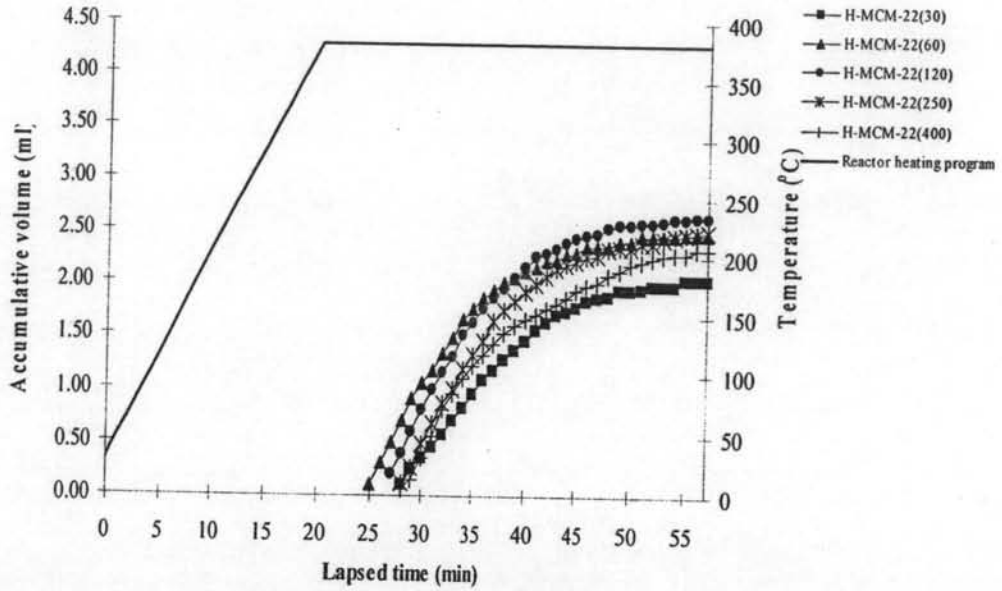

Figure 4.12 Accumulative volume of liquid fractions from catalytic cracking of PP waste over H-MCM-22 with various SiO_2/Al_2O_3 ratios at 380°C (Condition: 10%wt catalyst of PP waste, N_2 flow of 20 cm^3/min and reaction time of 40 min).

Figure 4.13 shows distribution of gas fraction obtained by catalytic cracking of PP waste over various H-MCM-22 catalysts at 380°C. In the presence of H-MCM-22(30) and H-MCM-22(60) catalysts provide the main product as n-butane, which are different from that H-MCM-22(120), H-MCM-22(250) and H-MCM-22(400) catalysts. The major product for higher SiO_2/Al_2O_3 ratios are C_5^+ > n-butane ≈ propene > i-butene.

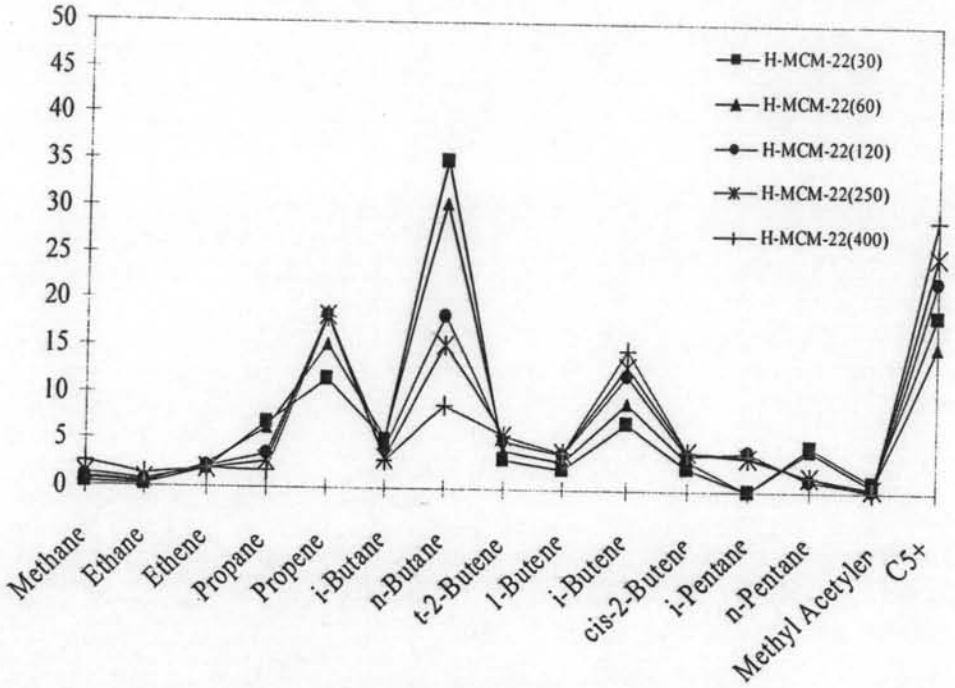

Figure 4.13 Distribution of gas fraction obtained by catalytic cracking of PP waste over H-MCM-22 with various SiO_2/Al_2O_3 ratios at 380°C (Condition: 10%wt catalyst of PP waste, N_2 flow of 20 cm^3/min and reaction time of 40 min).

Figure 4.14 shows product distribution of light oil obtained by catalytic cracking of PP waste over various H-MCM-22 catalysts at 380°C. The product distributions in liquid phase are affected by SiO_2/Al_2O_3 ratio in catalyst. From obtained data, the major product of H-MCM-22(30) and H-MCM-22(60) are distributed in the range of C_7 to C_9 but lower selectivity to C_6. For H-MCM-22(120), H-MCM-22(250) and H-MCM-22(400) contribute higher selectivity in the range of C_6-C_8. However, almost catalysts donate the similar high selectivity to C_7 and C_8 except the one with SiO_2/Al_2O_3 of 30 provides high selectivity to C_9 due to coke formation and Al in octahedral site.

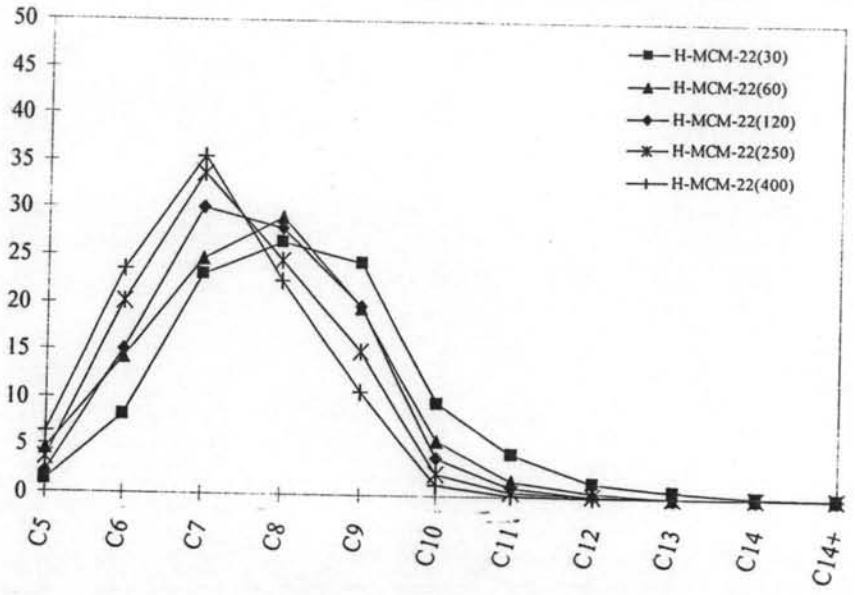

Figure 4.14 Carbon number distribution of distillated oil obtained by catalytic cracking of PP waste over H-MCM-22 with various SiO_2/Al_2O_3 ratios at 380°C (Condition: 10%wt catalyst of PP waste, N_2 flow of 20 cm^3/min and reaction time of 40 min).

The product distribution of SUPLECO GC standard gasoline is shown in Figure 4.15. It is found that the liquid distribution is in the range of C_7-C_8. That is comparable to the distillated oil obtained in this work based on the boiling point range using n-paraffins as reference. Hence, it can be concluded that H-MCM-22 catalysts with SiO_2/Al_2O_3 ratios 60 to 400 can be the good cracking catalyst for conversion PP waste to the valuable fraction of liquid hydrocarbon in the range of gasoline.

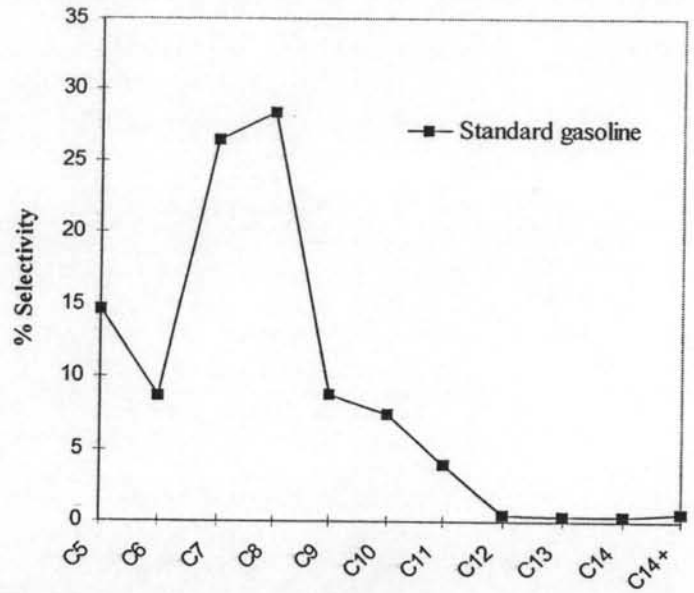

Figure 4.15 Carbon number distribution of commercial SUPELCO GC standard gasoline.

4.2.3 Effect of reaction temperature

The values of % conversion and the product yield for thermal cracking of PP waste and catalytic cracking over sample H-MCM-22(60) at various temperatures of 350, 380 and 400°C are shown in Table 4.5. H-MCM-22(60) catalyst is used for studying the effect of temperature on its activity. The thermal cracking in the absence of catalyst is test in comparison. Conversion values increase when reaction temperature increases from 350°C to 400°C. The activities of H-MCM-22(60) catalyst in PP waste cracking are in the range of 49-95 %. The conversion significantly affected by the temperature varied from 350-380°C. For all cases when considering the reaction at 380°C and 400°C, the main product is gas fraction at the yield 57% with minor product in liquid fraction at the yield about 35-39%. The amounts of residue reduce from 7.5 wt% to 5.2 wt% with wax about 3.6-4.9% and solid coke 1.6-2.6 %. In case of catalytic cracking of PP waste at 350°C, it cannot be calculated solid coke or wax value because plastic is melted and combined with catalyst remained in the reactor.

Table 4.5 Conversion and product yield from catalytic cracking of PP waste over H-MCM-22(60) with various temperatures (Condition: 10%wt catalyst of PP waste, N_2 flow of 20 cm^3/min and reaction time of 40 min)

	Temperature (°C)					
	350°C	380°C	400°C	Thermal Cracking 350°C	Thermal Cracking 380°C	Thermal Cracking 400°C
Conversion[a] (%)	49.40	92.47	94.80	2.33	23.60	65.67
Yield[b] (%)						
1. gas fraction	36.27	57.07	56.20	2.33	12.20	27.33
2. liquid fraction	13.13	35.40	38.60	-	11.40	38.33
- % distillated oil	34.91	63.80	51.48	-	54.87	52.17
-% heavy oil	65.10	36.20	48.52	-	45.13	47.83
3. residue	50.60	7.53	5.20	97.67	76.40	34.33
- wax	-	4.92	3.59	-	-	-
- solid coke	-	2.61	1.61	-	-	-
Total volume of liquid fraction (cm^3)	1.00	2.40	2.68	-	0.45	1.60
Liquid fraction density (g/cm^3)	0.66	0.74	0.72	-	0.72	0.74

[a] *Deviation within 0.40 %*

[b] *Deviation within 0.40 %*

Figure 4.16 shows the accumulative volume of liquid fraction in the graduated cylinder and the temperature of the reactor increase as a function of lapsed time. When the temperature is increased, the initial rate of liquid fraction formation is faster. The rate of liquid formation is in the order of 400°C > 380°C > 350°C and the highest total volume of liquid fraction is obtained for the 400°C.

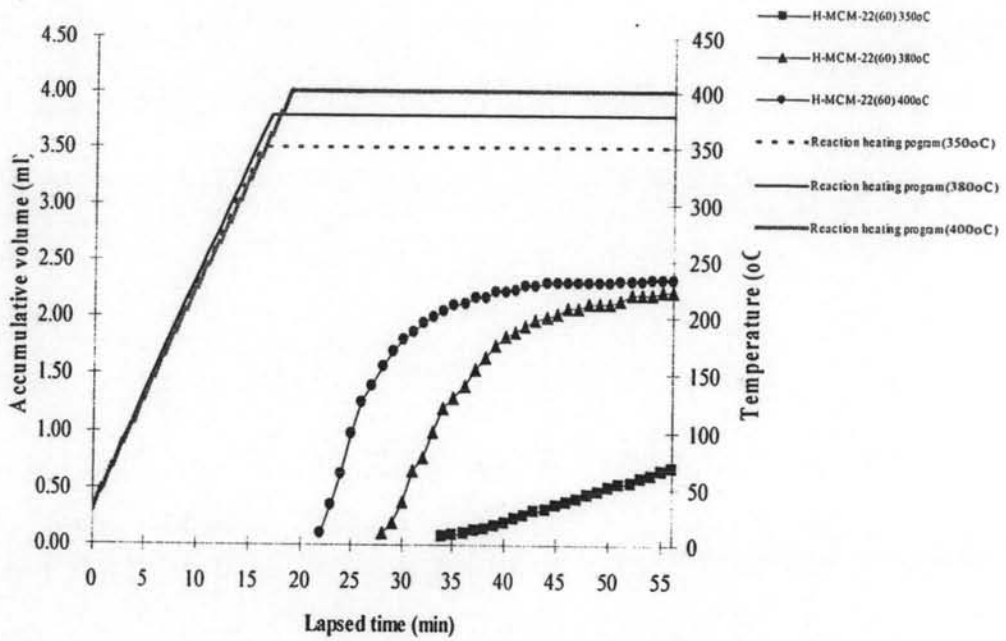

Figure 4.16 Accumulative volume of liquid fractions from catalytic cracking of PP waste over H-MCM-22(60) with various temperatures (Condition: 10%wt catalyst of PP waste, N_2 flow of 20 cm^3/min and reaction time of 40 min).

Figure 4.17 shows product distributions of gas fraction obtained by catalytic cracking of PP waste over H-MCM-22(60) catalyst at C_1 through C_5. Among gases products, formation of n-buntane, C_5^+, propene are favored. The major component for catalytic cracking is n-butane and C_5^+.

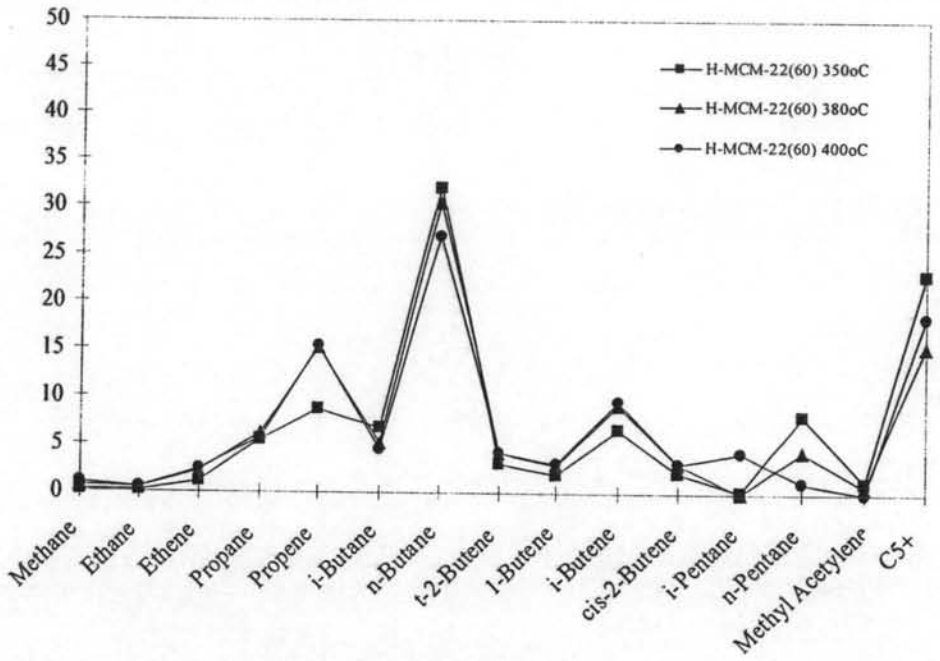

Figure 4.17 Distribution of gas fraction obtained by catalytic cracking of PP waste over H-MCM-22(60) with various temperatures (Condition: 10%wt catalyst of PP waste, N_2 flow of 20 cm^3/min and reaction time of 40 min).

Figure 4.18 shows product distribution of distillated oil obtained by H-MCM-22(60) at various reaction temperatures. The distillated oil components are mainly in the range of C_7 to C_8 at 380°C and 400°C, but C_8 is remarkable at reaction temperature 380°C. However, this change is not significant. Accordingly to the result of temperature affect on PP waste cracking, the temperature of 380°C is detected to be the test condition for further studies in this work because considerable of liquid fractions is obtained. When reaction temperature rising, the liquid fraction of lighter hydrocarbon C_6 increases while that of heavier hydrocarbon (C_8-C_9) decreases.

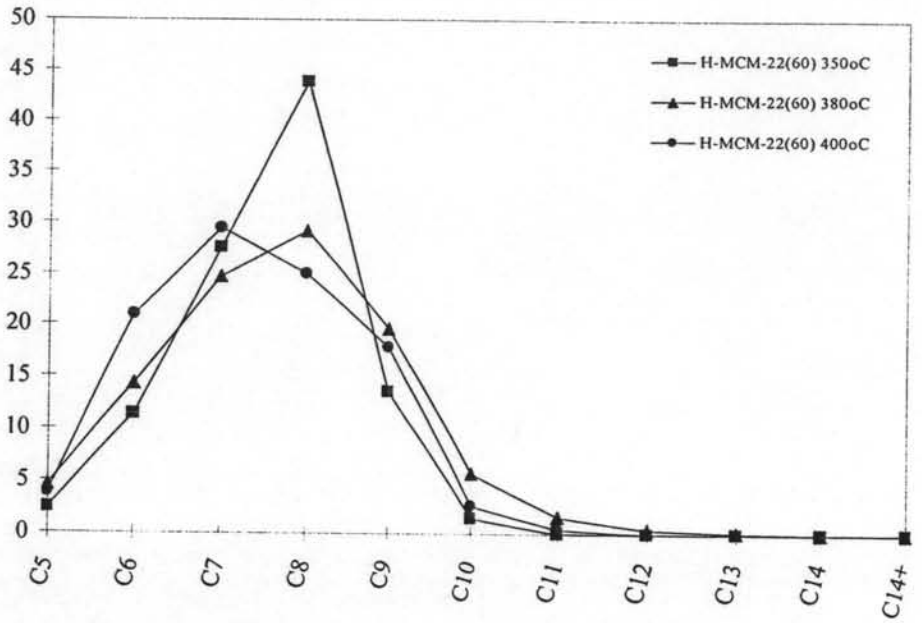

Figure 4.18 Carbon number distribution of distillated oil obtained by catalytic cracking of PP waste over H-MCM-22(60) with various temperatures (Condition: 10%wt catalyst of PP waste, N_2 flow of 20 cm^3/min and reaction time of 40 min).

4.2.4 Effect of polypropylene waste to catalyst ratio

The value of % conversion and product yield from PP waste cracking over H-MCM-22(120) at various catalyst amounts of 5wt%, 10wt% and 15wt% to PP waste are shown in Table 4.6. The highest conversion value of 92% is obtained in the case of using 10wt% but the conversion decreases to 89%, and 77% in the case of using 15wt% and 5wt% catalyst amount, respectively. The conversion strongly depends on the catalyst amount not exceeding 10wt%. However, the residue of 15wt% is higher than 10wt% catalytic amount. The excess amount of catalyst further makes the liquid fraction undergo cracking to smaller molecule in form of gas products. The residue produced by using 5wt% catalyst amount contains mainly wax due to lower activity compared to the case using higher amount of catalyst. Similarly to previous discussion in other cases, the lower activity, the higher wax or coke is found. The selectivity of distillated oil and heavy oil in liquid fraction is not significantly affected by the catalyst amount.

Table 4.6 Conversion and product yield from PP waste cracking over H-MCM-22 (120) with various catalyst amounts (Condition: N_2 flow of 20cm^3/min, 380°C and reaction time of 40 min)

	Catalyst amount to PP waste		
	5%	10%	15%
Conversion[a] (%)	76.73	91.60	89.27
Yield[b] (%)			
1. gas fraction	45.73	53.60	53.80
2. liquid fraction	31.00	38.00	35.47
- % distillated oil	58.04	55.63	60.31
-% heavy oil	41.95	44.38	39.69
3. residue	23.40	8.40	10.73
- wax	19.75	5.05	5.92
- solid coke	3.65	3.36	4.22
Total volume of liquid fraction (cm^3)	2.12	2.63	2.45
Liquid fraction density (g/cm^3)	0.73	0.72	0.73

[a] *Deviation within 0.40 %*

[b] *Deviation within 0.55 %*

Figure 4.19 shows the accumulated volume of liquid fraction obtained by catalytic cracking of PP waste over H-MCM-22 catalyst with various catalytic amounts at 380°C. It is found that the initial rate of liquid fraction formation is in order of 15wt% > 10wt% > 5wt% catalyst amount. The total volume of liquid fraction indicates that the amount of 5wt% catalyst providing only 2.12 cm^3 that is not enough to make maximum volume of liquid fraction while the excess catalyst amount is not beneficial on cracking increasing yield of liquid fraction more than 2.45 cm^3. The optimum catalyst amount is the 10wt% catalyst to PP waste the greatest total volume of liquid fraction of 2.63 cm^3.

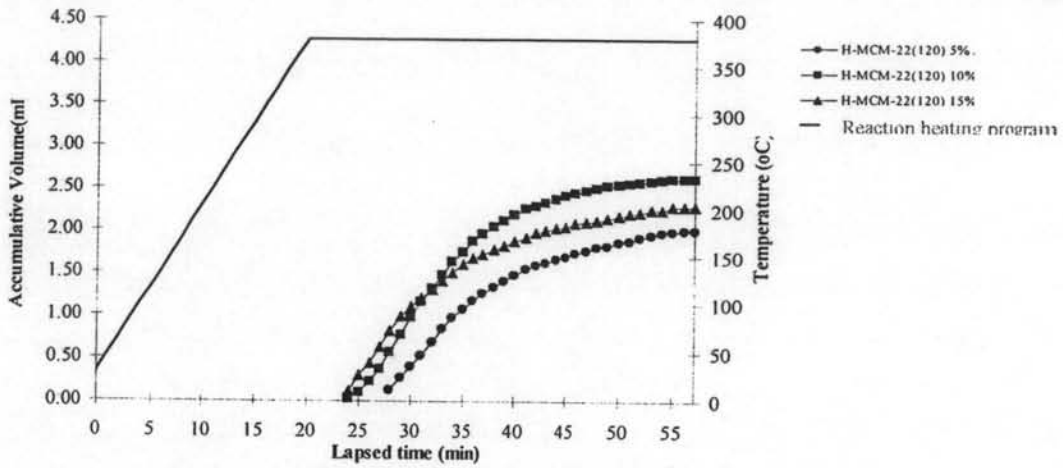

Figure 4.19 Accumulative volume of liquid fractions from from PP waste cracking over H-MCM-22(120) with various catalyst amounts at 380°C (Condition: N_2 flow of 20 cm^3/min and reaction time of 40 min).

Figure 4.20 shows distribution plots of gas product obtained by cracking of PP waste at 380°C with various catalyst amounts. The favored gaseous products are n-butane, propene, C_5^+ and i-butene. The selectivity of gas fraction for these catalysts are not significant different between them.

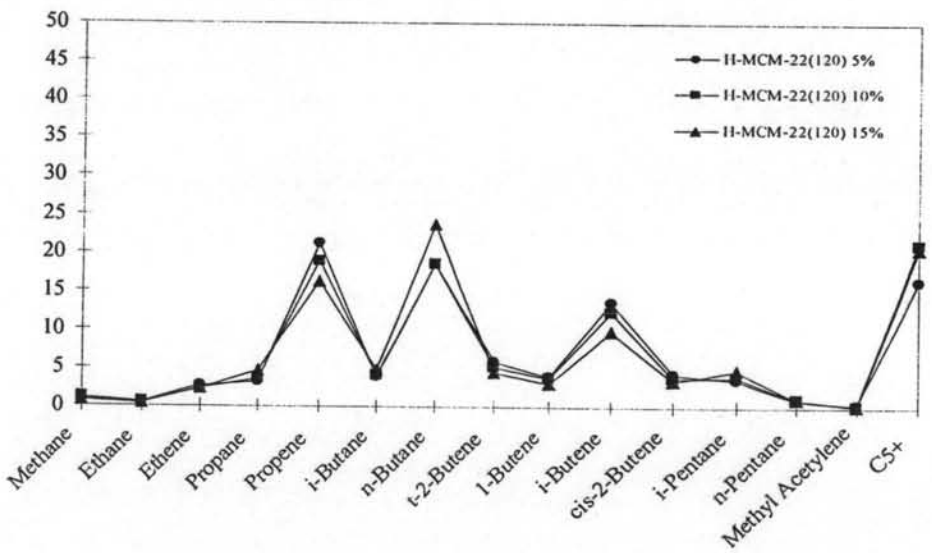

Figure 4.20 Distribution of gas fraction obtained by catalytic cracking of PP waste over H-MCM-22(120) with various catalyst amounts at 380°C (Condition: N_2 flow of 20 cm^3/min and reaction time of 40 min).

Figure 4.21 shows product distribution of distillate oil obtained by catalytic cracking of PP waste at 380°C with various catalyst amounts. There are no significant differences in distribution of liquid fraction. Using to 15wt% catalyst amount the selectivity to each liquid component in liquid fraction seems to be 5wt% that both 5wt% and 15wt% catalytic amounts provide mainly C_7 to C_8 range in liquid fraction. For 10wt% amount of catalyst, the liquid fraction is mainly C_7 to C_9. It can be explained by the effect of catalyst amount but the relation is not in sequence due to vary wide range of varied values. It may be in sequence in a specific range of catalyst amount less than 10wt%. Thus the wide range distribution of product depends on the catalyst amount; the choice depends on what type of product is required. In this study, the choice is using 10wt% catalyst amount according to the highest yield of liquid fraction.

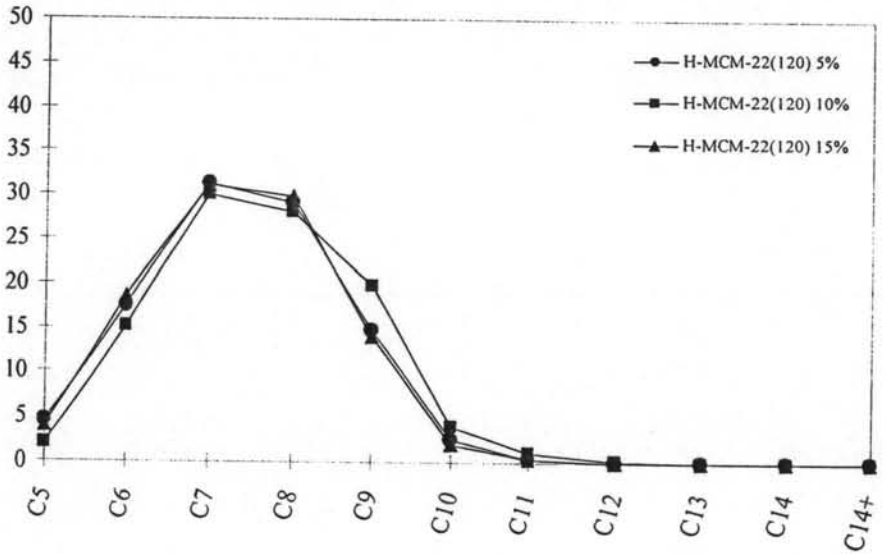

Figure 4.21 Carbon number distribution of distillated oil obtained by catalytic cracking of PP waste over H-MCM-22(120) with various catalyst amounts at 380°C (Condition: N_2 flow of 20 cm^3/min and reaction time of 40 min).

4.3 Characterization and catalytic activity of del-H-MCM-22 catalysts

4.3.1 Characterization of del-H-MCM-22 catalysts

4.4.1.1 XRD results

The delamination process of MCM-22(P) by swollen reagent is articulated in different treatment steps:

- swelling of MCM-22(P) sample at 80°C by CTMABr, TPAOH and H_2O (swollen product);
- ultrasound treatment (sonicated product);
- calcination (final product del-MCM-22).

The structure change during the delaminating treatment was followed by XRD technique. The XRD pattern of swollen product Figure 4.2(c) does not show the [001] peak at $2\theta \approx 3$ while the [002] peak at $2\theta \approx 7$ shifts to lower 2θ value. This result indicates that the basic TPAOH can cleave the linkages between layers and makes the surfactant molecules easily enter into the layer, resulting in the formation of material with expanded layers. Moreover, the solubilization of the SiO_4^- species causes the partial destruction of the zeolite framework. By calcination, organic molecules are removed, and the expanded layer structure seriously collapses. It can be seen in Figure 4.22(d), which shows broader peaks and lower intensity than calcined MCM-22 (Figure. 4.22(a)).

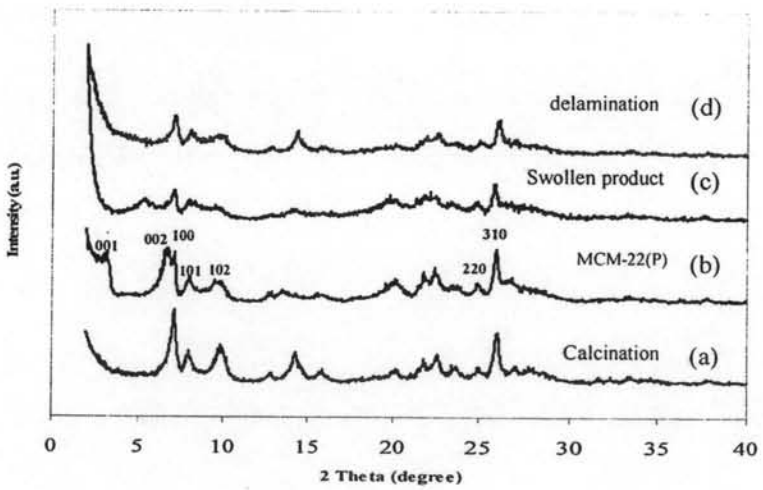

Figure 4.22 XRD patterns of (a) calcined MCM-22, (b) MCM-22(P), (c) swollen product before sonication and (c) del-H-MCM-22.

Figure 4.23 gives the XRD patterns of del-MCM-22 samples, prepared by using different amount of TPAOH base, the important factor. The diffraction line decreases in intensity with increasing TPAOH content. When the weight ratio of TPAOH aqueous solution (20.10%) to the as-synthsized MCM-22 is about 12. The intensity of diffraction line in the XRD pattern of del-MCM-22 obviously decreases, which denoted as D4 in Figure 4.23(e). It provides the highest external surface area in Table 4.7. The suitable condition was 1.00 g MCM-22(P): 11.90 g H_2O: 5.64 g CTMABr: 12.02 g TPAOH and sonicated for 5 h modified by Jung *et al.* [38]. Figure 4.24 shows XRD patterns of del-H-MCM-22 with SiO_2/Al_2O_3 ratios of 30 and 60 by above optimum condition.

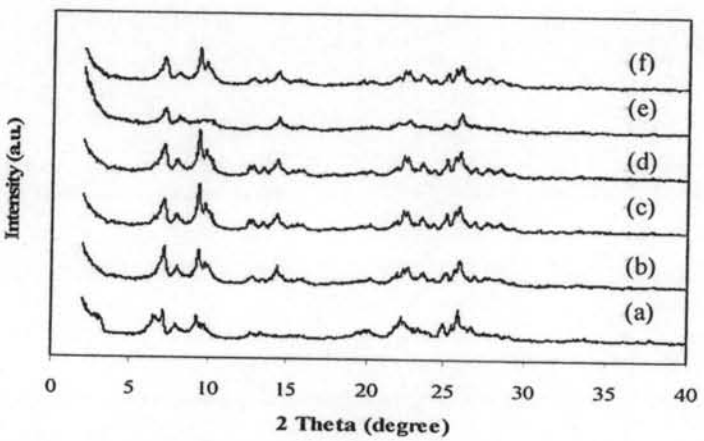

Figure 4.23 XRD patterns of del-MCM-22 samples with various conditions; (a) MCM-22(P), (b) D1, (c) D2, (d) D3, (e) D4 and (f) D5.

Table 4.7 Textural properties of del- MCM-22 samples with various conditions

Sample	Total specific sureface area[a] (m^2/g)	External surface area[b] (m^2/g)	Micropore distribution[c] (nm.)	Micropore volume[b] (cm^3/g)
D1	510	133	0.60	117.13
D2	502	164	0.60	115.32
D3	507	143	0.60	116.38
D4	599	197	0.60	137.63
D5	521	106	0.60	119.74

[a] *Calculated using the BET plot method,*

[b] *Calculated using the t- plot method,*

[c] *Calculated using the MP- plot method*

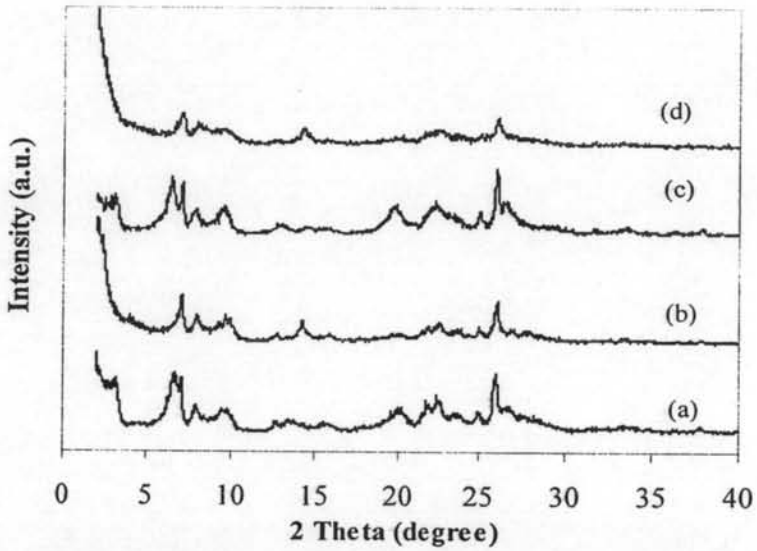

Figure 4.24 XRD patterns of (a) As-synthesized MCM-22(30), (b) del-H-MCM-22(30), (c) As-synthesized MCM-(60), and (d) del-H-MCM-22(60) catalysts.

4.4.1.2 SEM Images of del-MCM-22 catalysts

Figure 4.25 illustrates SEM images of H-MCM-22 catalysts (Figure 4.25(a), (b)) and delaminated MCM-22 catalysts (Figure 4.25(c), (d)). The del-MCM-22 does not exhibit the typical platelet morphology of MCM-22(P) crystal, but shows exfoliated shape. The delaminated catalysts have smaller particle size than H-MCM-22 catalysts.

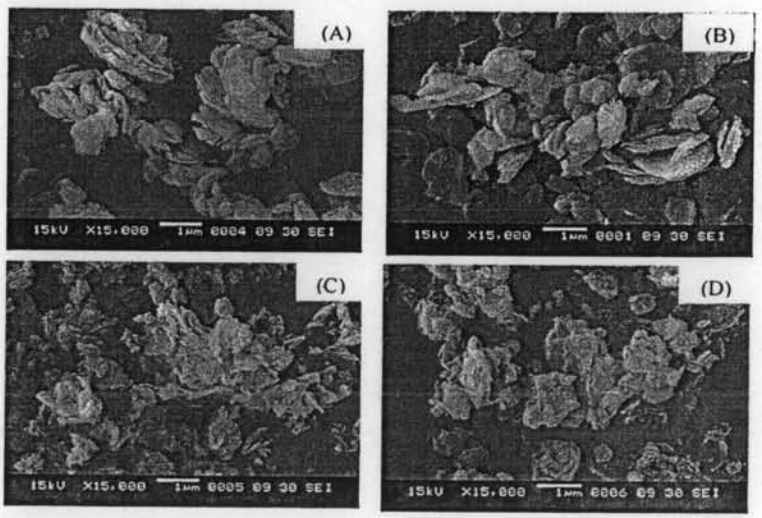

Figure 4.25 SEM images of calcined sample (A) H-MCM-22(30), (B) H-MCM-22(60), (C) del-H-MCM-22(30) and (D) del-H-MCM-22(60).

4.4.1.3 ^{27}Al-MAS-NMR Spectra

Figure 4.26 and 4.27 show the ^{27}Al-MAS-NMR spectra of H-MCM-22 samples compared and del-H-MCM-22 samples with SiO_2/Al_2O_3 of 30 and 60, respectively. It is observed that the del-H-MCM-22 sample shows slightly lower intensity at 0 ppm signal than H-MCM-22 sample. The relative amounts of the tetrahedral (T) and octahedral (O) aluminum atoms are I_T/I_O = 1: 0.20 and 1: 0.18, for del-H-MCM-22(30) and H-MCM-22(30), respectively. The I_T/I_O of del-H-MCM-22(60) and H-MCM-22(60) samples are the same values, i.e. 1: 0.17.

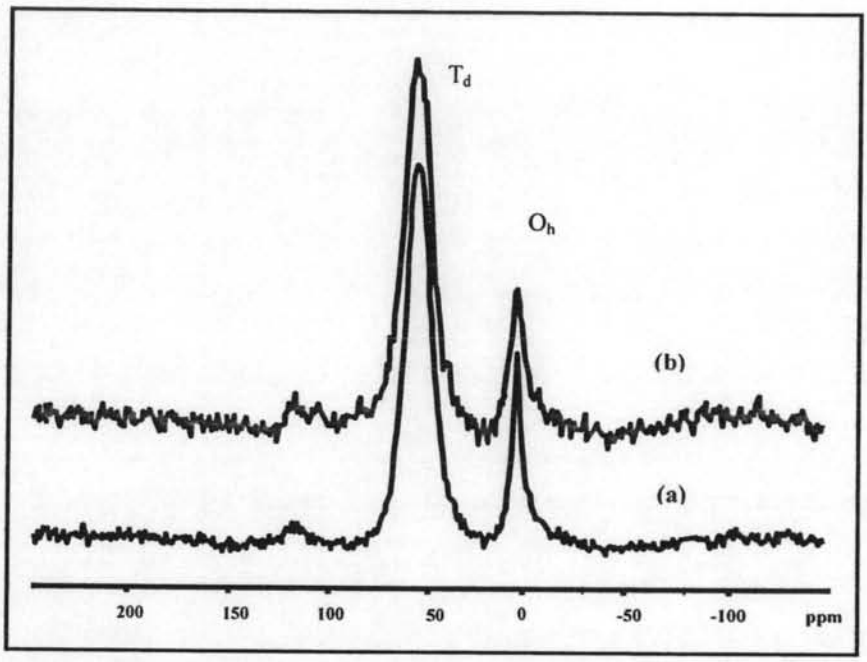

Figure 4.26 The ^{27}Al-MAS-NMR Spectra of (a) H-MCM-22(30), (b) del-H-MCM-22(30).

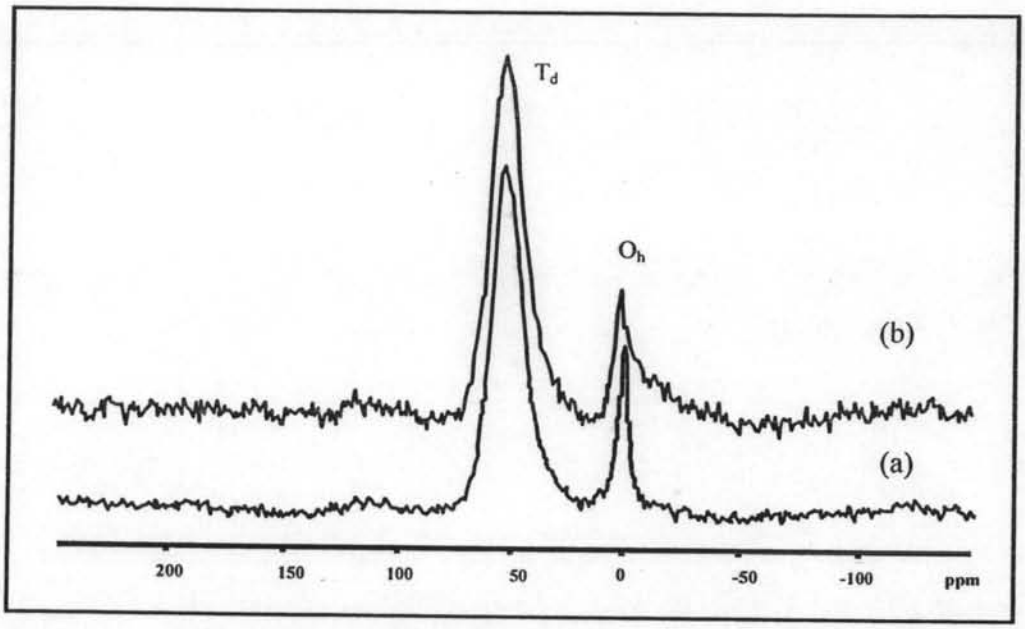

Figure 4.27 The ^{27}Al-MAS-NMR Spectra of (a) H-MCM-22(60), del-H-MCM-22(60).

4.4.1.5 Sorption properties of del-MCM-22 catalysts

The N_2 adsorption-desorption isotherms of the calcined del-H-MCM-22(30) and del-H-MCM-22(60) are shown in Figure 4.28. All samples exhibit a type I isotherm which is typical for microporous material. Textural properties of calcined H-MCM-22 and del-H-MCM-22 catalysts are compared in Table 4.8. The del-H-MCM-22(60) provides the highest external surface area (455 m^2/g) while the external surface area of del-H-MCM-22(30) is 205 m^2/g. The pore size distribution number, obtained from adsorption data, is 0.6 for all del-MCM-22 catalysts.

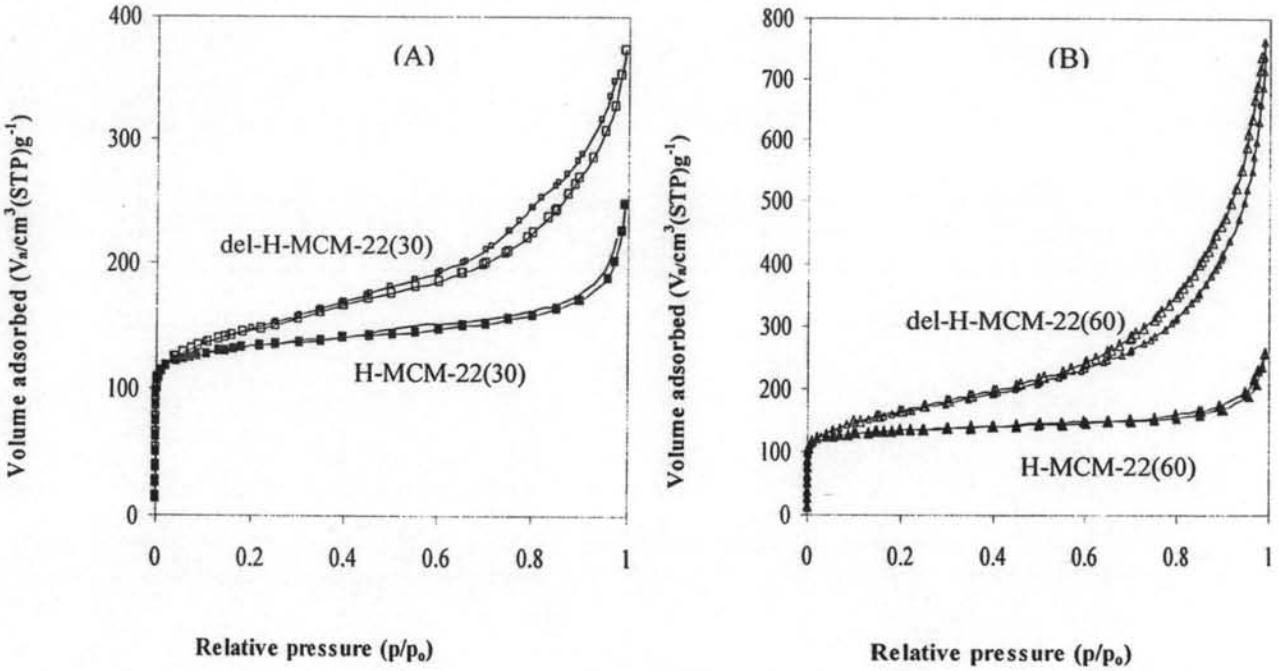

Figure 4.28 N_2 adsorption-desorption isotherms of H-MCM-22(30) and del-H-MCM-22(30) (A) compared with H-MCM-22(60) and del-H-MCM-22(60) catalysts (B).

Table 4.8 Textural properties of calcined del-H-MCM-22 catalysts compared with H-MCM-22

Sample	Total specific sureface area[a] (m^2/g)	External surface area[b] (m^2/g)	Micropore distribution[c] (nm)	Micropore volume[b] (cm^3/g)
H-MCM-22 (30)	487	60	0.60	0.18
H-MCM-22 (60)	540	56	0.60	0.21
del H-MCM-22 (30)	530	205	0.60	0.12
del-H-MCM-22 (60)	580	455	0.60	0.04

[a]Calculated using the BET plot method,

[b]Calculated using the t- plot method,

[c]Calculated using the MP- plot method

4.4.1.6 Acidity of del-MCM-22 catalysts

Figure 4.29 and Figure 4.30 show ammonia TPD profile of Na-form, H-form and delaminated MCM-22 with SiO_2/Al_2O_3 ratio 30 and ratio 60, respectively. The peak contented lower than 200°C is typically assigned to a weaker acid site, and the other on at 350°C is assigned to a strong acid site. For delaminated samples, the numbers of weaker acid sites decrease according to the decrease in aluminum content in catalyst.

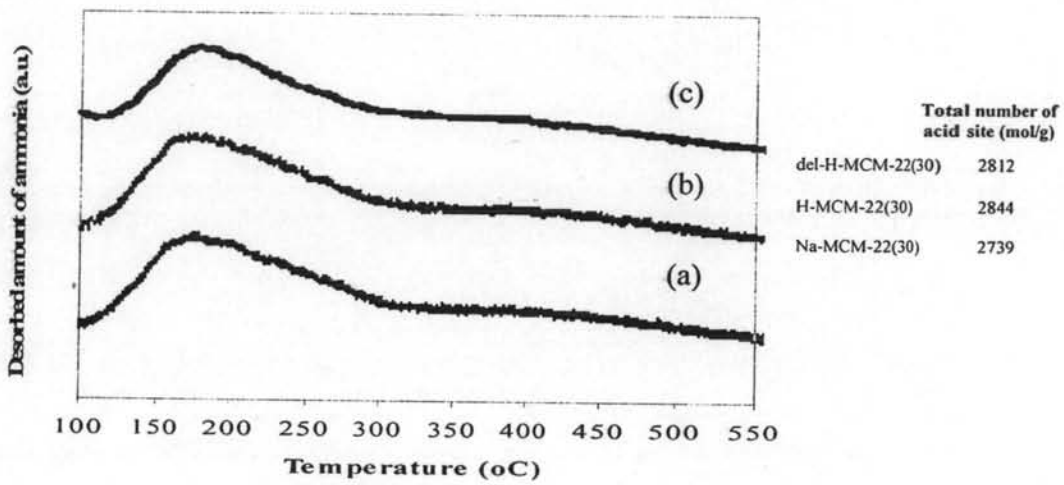

Figure 4.29 Ammonia TPD profile of (a) Na-MCM-22(30), (b) H-MCM-22(30) and (c) del-H-MCM-22(30).

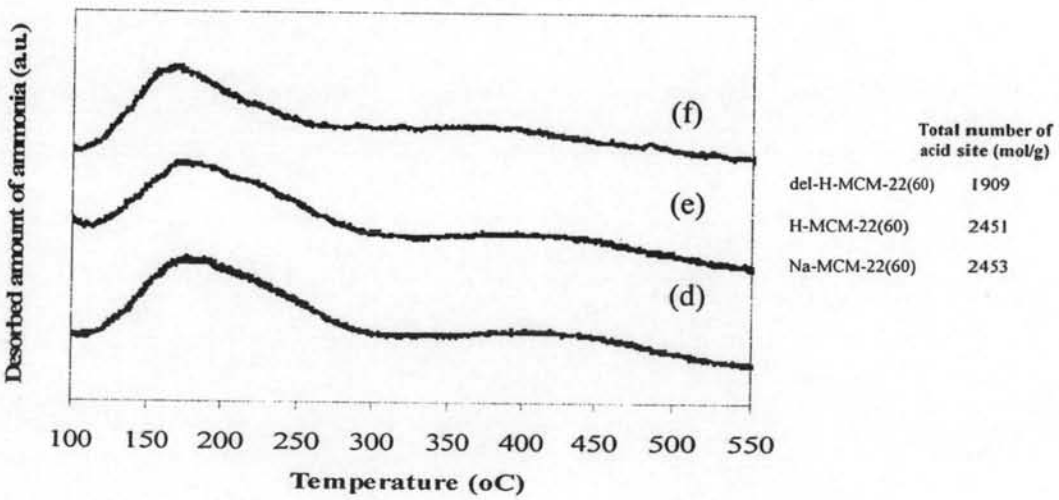

Figure 4.30 Ammonia TPD profile of (d) Na-MCM-22(60), (e) H-MCM-22(60) and (f) del-H-MCM-22(60).

4.3.2 Activity of del-H-MCM-22 catalysts

The values of % conversion and the product yield for catalytic cracking of PP waste over del-H-MCM-22(30) and del-H-MCM-22(60) catalysts at 380°C are shown in Table 4.9. The del-H-MCM-22(30) provides relatively higher yield of gas fraction and lower residue (wax) comparing to H-MCM-22(30) while yield of liquid fraction and the amount of solid coke are not significantly different between them. The number of acid site, determined by NH_3-TPD method, can not be explained the activity of those catalysts because activities do not relate to the change in active site. The high external surface area is accounted for its activity. The del-H-MCM-22(30) has higher external surface area (205 m^2/g) than H-MCM-22(30) (60 m^2/g) while the numbers of acidity are not significant different between them. Therefore, del-H-MCM-22(30) provides higher yield of gas fraction than H-MCM-22(30). This effect is pronounced for the case of high external surface area. This observation correlates well with the catalytic activity for processing a large molecule which cannot diffuse within the micropores and can react at the external surface.

The del-H-MCM-22(60) presents the highest external surface area, but the delamination step is favored by decreasing aluminum content of parent materials [40]. This effect is more significant decreasing acidity of delaminted catalyst. This impact cause the value of % conversion in the case of del-H-MCM-22(60) and H-MCM-22(60) are not different due to the balance between acid amount and external surface area. The significant differences are gas product and solid coke, del-H-MCM-22(60) provides lower amount of gas product and solid coke comparing to the H-MCM-22 (60) catalyst.

The conversion value and the product yield are obtained by the catalytic cracking of PP waste over delaminated catalysts at 380°C. The del-H-MCM-22(60) catalyst performs higher % conversion, liquid fraction and lower residues than del-H-MCM-22(30).

Table 4. 9 Conversion and product yield from PP waste cracking over H-MCM-22 and del-H-MCM-22 catalysts at 380°C (Condition: 10 wt% catalyst of plastic, N_2 flow of 20 cm^3/min, 380°C and reaction time of 40 min).

	Catalyst			
	Del-H-MCM-22 (30)	H-MCM-22 (30)	Del-H-MCM-22 (60)	H-MCM-22 (60)
Conversion[a] (%)	87.70	81.50	92.70	92.47
Yield[b] (%)				
1. gas fraction	57.40	52.20	55.60	57.07
2. liquid fraction	30.30	29.30	37.10	35.40
- % distillated oil	60.39	64.97	60.88	63.80
-% heavy oil	39.61	35.03	39.12	36.20
3. residue	12.30	18.50	7.30	7.53
- wax	6.85	13.02	5.38	4.92
- solid coke	5.46	5.48	1.93	2.61
Total volume of liquid fraction (cm^3)	2.15	1.98	2.63	2.40
Liquid fraction density (g/cm^3)	0.71	0.74	0.71	0.74

[a] *Deviation within 0.60 %*

[b] *Deviation within 0.50 %*

Figure 4.31 shows the accumulative volume of liquid fractions in the graduated cylinder and the temperature of reactor increases as a function of lapsed time. The initial rate of liquid fraction formation, there is not significant difference between H-MCM-22 and del-H-MCM-22 catalysts. The del-H-MCM-22 (60) is obviously faster than the del-H-MCM-22(30). Therefore, the total volumes of these two catalysts are different. This is due to the effect of surface area and the acidity of catalyst.

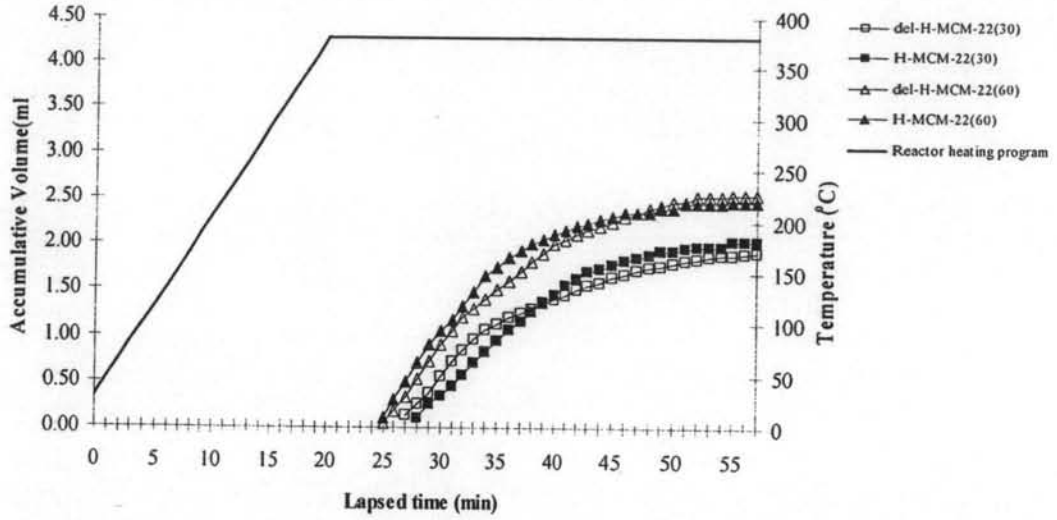

Figure 4.31 Accumulative volume of liquid fractions from PP waste cracking over H-MCM-22 and del-H-MCM-22 catalysts at 380°C (Condition: 10 wt% catalyst of plastic, N_2 flow of 20 cm^3/min and reaction time of 40 min).

Figure 4.32 shows distribution of gas fraction obtained by catalytic cracking of PP waste over del-H-MCM-22 and H-MCM-22 catalysts at 380°C. The major component for H-MCM-22 catalyst is n-butane more than C_5^+. While del-H-MCM-22 catalysts provide the selectivity of C_5^+ nearly amount as n-butane in case of del-H-MCM-22 (30) and exhibit higher amount of C_5^+ in case of del-H-MCM-22(60).

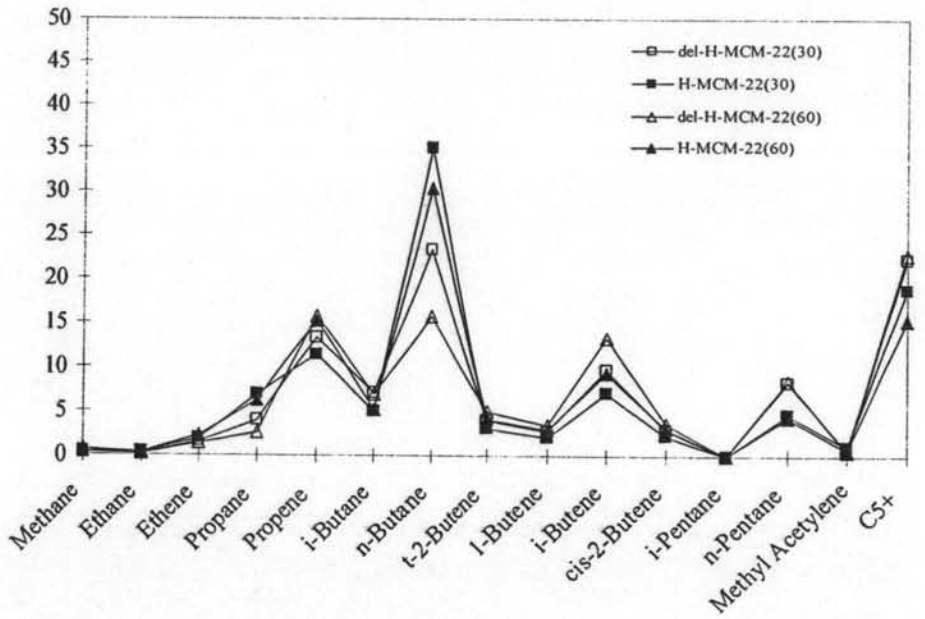

Figure 4.32 Distribution of gas fraction obtained by catalytic cracking of PP waste over H-MCM-22 and del-H-MCM-22 catalysts at 380°C (Condition: 10 wt% catalyst of plastic, N_2 flow of 20 cm^3/min and reaction time of 40 min).

Figure 4.33 shows product distribution of distillated oil obtained by catalytic cracking of PP waste over H-MCM-22 and del-H-MCM-22 catalysts at 380°C. The distillated oil components of H-MCM-22 catalysts are in the range of C_7 to C_9 while delaminated catalysts provide in the range of C_6 to C_8.

For the PP waste cracking over sample del-H-MCM-22(30), the liquid fraction is rich C_7 and C_8. When the highest external surface area del-H-MCM-22(60) is used as catalyst, the liquid fraction is mainly C_7 components because high external surface area causes the increase of the selectivity to lighter liquid hydrocarbon.

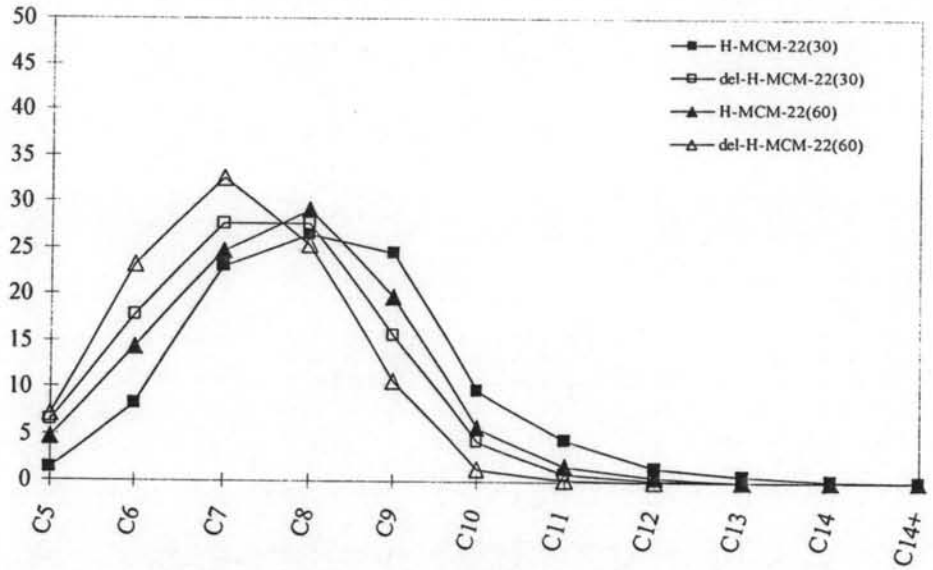

Figure 4.33 Carbon number distribution of distillated oil obtained by catalytic cracking of PP waste over H-MCM-22 and del-H-MCM-22 catalysts at 380°C (Condition: 10 wt% catalyst of plastic, N_2 flow of 20 cm^3/min, 380°C and reaction time of 40 min).

4.4 Recycle of catalysts

4.2.1 Characterization of regenerated type I and type II catalysts

4.2.1.1 XRD results

The surface and pores of used H-MCM-22(120) catalyst are blocked after first run reaction, due to coke deposition. In this work, the spent catalyst is washed with hexane for several times, and dried at 80°C overnight, then calcined at 540°C for 8 h, which denoted as regenerated type I. In addition, the regenerated type I is treated with 1 M NH_4Cl solution for 2 h, 5 times and washed with DI water to remove Cl ion, dried at 80°C overnight then calcined at 540°C for 8 h, which denoted as regenerated type II. Figure 4.34 shows XRD patterns of fresh, regenerated type I and regenerated type II catalysts. Two XRD patterns of these regenerated catalysts confirm a characteristic XRD patterns like fresh MCM-22 catalyst. The intensity of [100] peak at $2\theta \approx 7$ of the regenerated catalysts decreases because the catalytic structure is partially deformed during reaction and regeneration via coke burning at elevated temperature 540°C or NH_4Cl treatment.

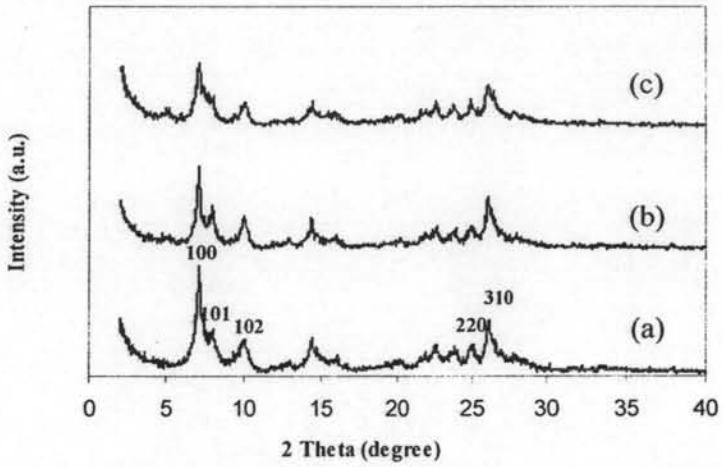

Figure 4.34 XRD patterns of (a) fresh H-MCM-22(120), (b) regenerated type I and (c) regenerated type II.

4.4.1.2 SEM Images of fresh and regenerated catalysts

In Figure 4.35 shows SEM images of fresh H-MCM-22 catalysts (A), regenerated type I (B), and regenerated type II (C) catalysts, respectively. Most particles have exfoliated shape. The regenerated catalysts are the same particle size as the fresh catalyst.

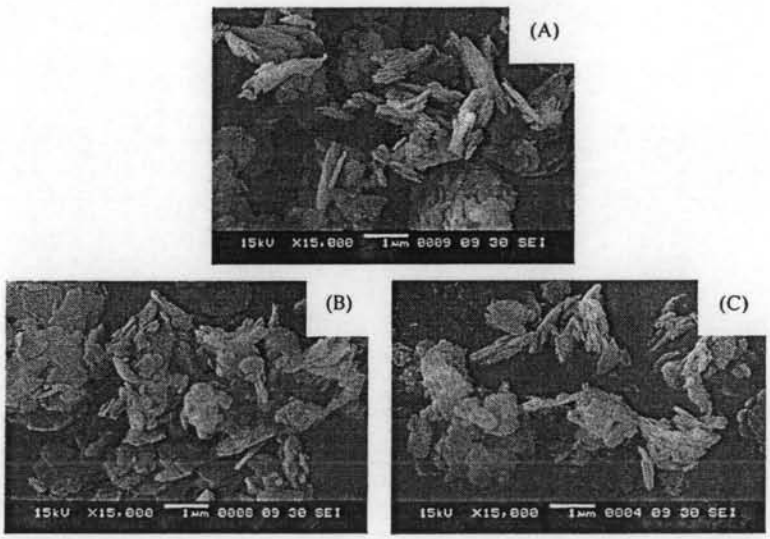

Figure 4.35 SEM images of calcined (A) fresh H-MCM-22(120), (B) regenerated MCM-22(120) type I and (C) regenerated MCM-22(120) type II catalysts.

4.4.1.3 Sorption properties regenerated catalysts

The adsorption-desorption isotherms of those catalysts are shown in Figure 4.36. The regenerated catalysts display the characteristic isotherm of micropore material with the specific surface area is slightly reduced by 12% for regenerated type I and 17% for regenerated type II as compared to the fresh one. Textural properties of fresh H-MCM-22 and regenerated MCM-22(120) catalysts are shown in Table 4.10. External surface area values of two regenerated catalysts show increasing from 41 to 44 and 54 due to the dispersion of exfoliated sheets of regenerated samples. On the other hands, decreasing of micropore volume is occurred because coke deposition still remains in regenerated catalysts.

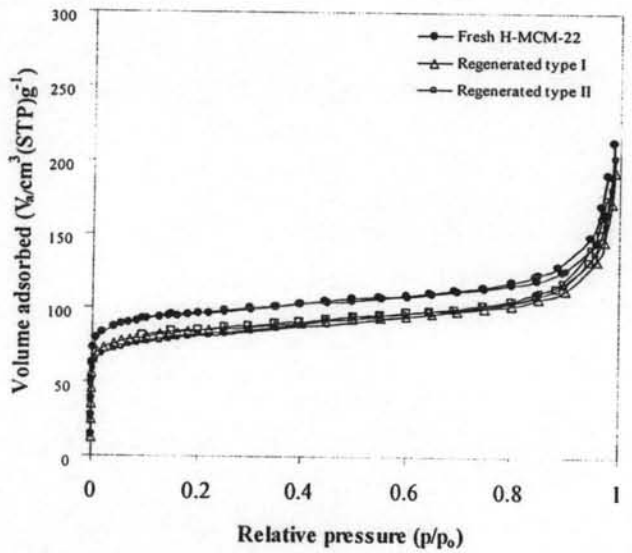

Figure 4.36 N_2 adsorption-desorption isotherms of fresh H-MCM-22(120) and regenerated MCM-22(120) catalysts.

Table 4.10 Textural properties of calcined regenerated MCM-22 catalysts.

Sample	Total specific sureface area[a] (m^2/g)	External surface area[b] (m^2/g)	Micropore distribution[c] (nm)	Micropore volume[b] (cm^3/g)
H-MCM-22 (120)	362	41	0.6	0.14
Regenerated type I	319	44	0.6	0.12
Regenerated type II	302	54	0.6	0.11

[a] *Calculated using the BET plot method,*

[b] *Calculated using the t- plot method,*

[c] *Calculated using the MP- plot method*

4.4.2 Activity of regenerated type I and type II

The values of % conversion and % yield obtained by PP waste cracking, using fresh, regenerated type I and regenerated type II of MCM-22(120) catalysts at 380°C are shown in Table 4.11. The values of % conversion are not significantly different between regenerated catalysts. The differences are the yield of gas fraction, light oil and heavy oil. The regenerated type I and regenerated type II catalysts provide relatively lower yield of gas fraction compare to the fresh catalyst. While total yield of liquid fraction and amount of solid coke are not different between them.

Lower yield of light oil and higher yield of heavy oil are obtained for the regenerated type I catalyst. While the regenerated type II catalyst provides slightly lower yield of distillated oil and higher yield of heavy oil than the fresh catalyst. This result suggests the regenerated catalyst have a lower surface area and acidity than the fresh catalyst. The conversion is decreased from 92% for fresh catalyst to 85% with for regenerated catalyst. Relatively more amount of residue, especially in form of wax was remained in the reactor of the regenerated catalyst than fresh catalyst.

Table 4.11 Conversion and product yield from PP waste cracking over fresh, regenerated MCM-22(120) type I and type II catalysts (Condition: 10%wt catalyst of PP waste, N_2 flow of 20 cm^3/min, 380°C and reaction time of 40 min)

	Fresh H-MCM-22(120)	Regenerated MCM-22(120) type I	Regenerated MCM-22 (120) type II
Conversion[a] (%)	91.60	84.70	85.40
Yield[b] (%)			
1. gas fraction	53.60	47.00	49.10
2. liquid fraction	38.00	37.70	36.30
- % distillated oil	57.99	48.74	53.01
-% heavy oil	42.01	51.27	46.99
3. residue	8.40	15.30	14.60
- wax	5.05	11.30	10.43
- solid coke	3.36	4.00	4.17
Total volume of liquid fraction (cm^3)	2.63	2.65	2.58
Liquid fraction density (g/cm^3)	0.73	0.73	0.71

[a]Deviation within 0.70 %

[b]Deviation within 0.60 %

Figure 4.37 shows the accumulative volume of liquid fraction in the graduated cylinder. The rates of liquid fraction formation are not significantly different between the fresh or regenerate type II catalysts while regenerated type I is slightly slower than them. The total volume of liquid fraction is not different between regenerated type I and regenerated type II catalysts while higher volume is obtained for fresh catalyst. The results lead to the conclusion that the regenerated catalysts exhibit lower efficiency after calcination or NH_4Cl treatment.

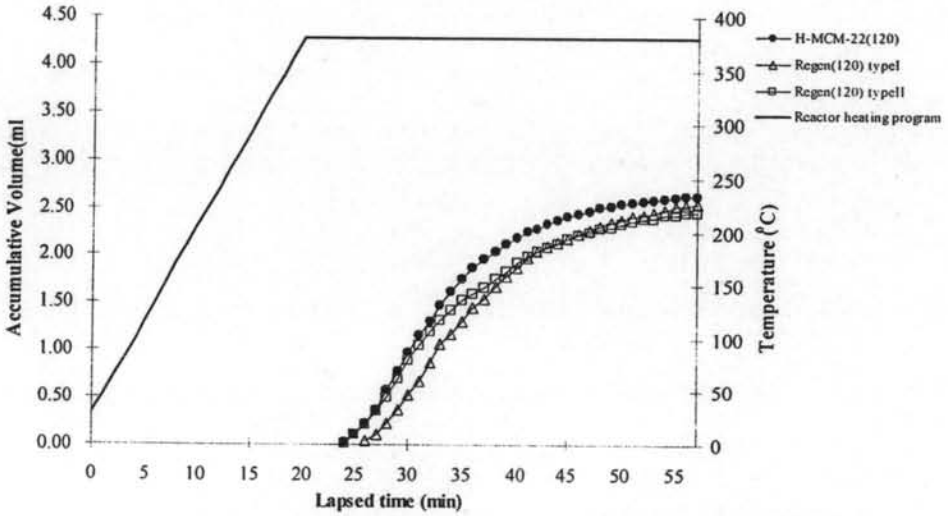

Figure 4.37 Accumulative volume of liquid fractions from PP waste cracking over fresh and the regenerated MCM-22(120) catalysts at 380°C (Condition: 10 wt% catalyst of plastic, N_2 flow of 20 cm^3/min and reaction time of 40 min).

Figure 4.38 shows distribution of gas fraction obtained by the PP waste cracking using the fresh and regenerated MCM-22(120) catalysts at 380°C. The gas fraction composes the same product distribution. There are no differences in the selectivity in gas fraction between the two regenerated catalysts while the fresh catalyst provides the favored n-butane product more than regenerated catalysts.

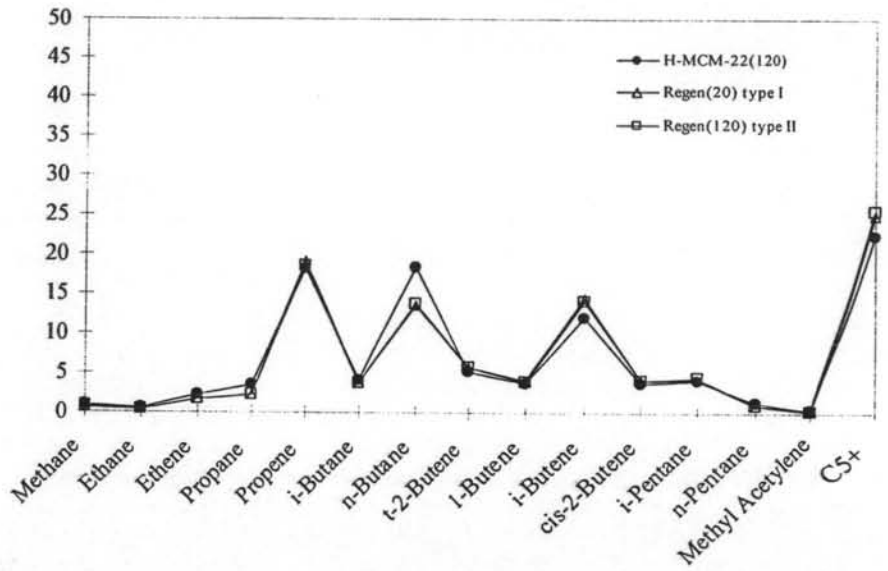

Figure 4.38 Distribution of gas fraction obtained by catalytic cracking of PP using the fresh and the regenerated MCM-22(120) catalysts at 380°C (Condition: 10 wt% catalyst of plastic, N_2 flow of 20 cm^3/min, and reaction time of 40 min).

Figure 4.39 shows product distribution of liquid fraction obtained by the PP waste cracking using fresh and regenerated catalysts. Both fresh and regenerated catalysts provide mainly C_7 to C_8 range in liquid fraction. The selectivity to C_9 using fresh catalyst is relatively higher than the regenerated catalysts. However, the selectivity to light oil (C_6-C_7) increases when regenerated catalysts are used.

The total volume of liquid fraction is about the same for fresh and regenerated catalysts. MCM-22(120) is stable for use as cracking catalyst and the used catalyst can be regenerated easily in a furnace. The cracking activity shows a few changes to 5% lower conversion.

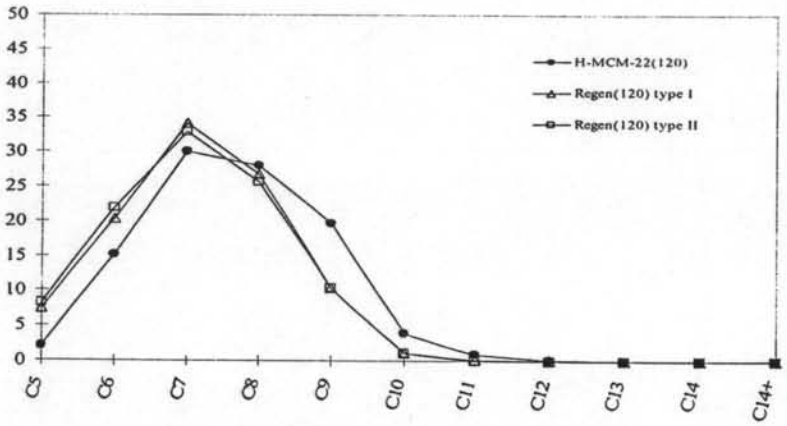

Figure 4.39 Carbon number distributions of liquid fraction obtained by catalytic cracking of PP waste using the fresh and the regenerated MCM-22(120) catalysts at 380°C (Condition: 10 wt% catalyst of plastic, N_2 flow of 20 cm^3/min, and reaction time of 30 min).

4.5 Catalytic activity of H-MCM-22 in HDPE waste cracking

4.5.1 Effect of reaction temperature and SiO_2/Al_2O_3 ratio

The values of % conversion and % yield for thermal cracking and catalytic cracking of HDPE waste over H-MCM-22 catalysts at two temperatures are shown in Table 4.12. Increasing temperature from 380°C to 400°C, catalytic cracking provides extremely higher % conversion and % yield of product than thermal cracking. For catalytic cracking, the value of HDPE waste conversion increases about 10% from 84% - 94% while the amount of residue decreases about 10%. This result indicated the residue is decomposed to gas and liquid products. For the thermal cracking at both reaction temperatures, no liquid fraction is found in the graduated cylinder. The result shows the difficultly in degradation of HDPE waste without catalyst at the temperature about 400°C or less. For such a case, the total weight loss of plastic after reaction is devoted to gas fraction.

The H-MCM-22(60) and H-MCM-22(120) catalysts are used for studying the effect of SiO_2/Al_2O_3 ratio in HDPE waste cracking. Considering data at the same temperature, the increasing of SiO_2/Al_2O_3 ratios from 60 to 120 is found that % conversion, % yield and residue are not different between them.

Table 4.12 Conversion and product yield from catalytic cracking of PE waste over H-MCM-22(60) and H-MCM-22(120) with two temperatures. (Condition: 10%wt catalyst of PE waste, N_2 flow of 20 cm^3/min and reaction time of 40 min)

	Temperature (°C)					
	380°C		400°C		Thermal Cracking 380°C	Thermal Cracking 400°C
	60	120	60	120		
Conversion[a] (%)	85.00	83.60	94.70	94.60	0.06	3.00
Yield[b] (%)						
1. gas fraction	62.40	60.20	67.10	64.20	0.06	3.00
2. liquid fraction	22.60	23.40	27.60	30.40	-	-
- % distillated oil	78.21	79.02	76.89	76.68	-	-
-% heavy oil	21.79	20.98	23.11	23.32	-	-
3. residue	15.00	16.40	5.30	5.40	99.40	97.00
- wax	12.69	12.98	3.67	3.86	-	-
- solid coke	2.31	3.42	1.63	1.54	-	-
Total volume of liquid fraction (cm^3)	1.65	1.70	2.00	2.24	-	-
Liquid fraction density (g/cm^3)	0.68	0.69	0.69	0.68	-	-

[a] *Deviation within 0.40 %*

[b] *Deviation within 0.50 %*

Figure 4.40 shows the accumulative volume of liquid fraction formation in the graduated cylinder obtained by the catalytic cracking of HDPE waste over H-MCM-22 catalyst two temperatures. In case of catalytic cracking, the initial rate of 400°C is much faster than 380°C according to the temperature dependence of kinetic effect.

The rate of liquid fraction formation for HDPE waste cracking over sample H-MCM-22(60) at 380°C is faster than that over sample H-MCM-22(120). That confirms the acidity effect of aluminum incorporated in the MCM-22 structure can play important role on activity of the catalysts in cracking of HDPE waste.

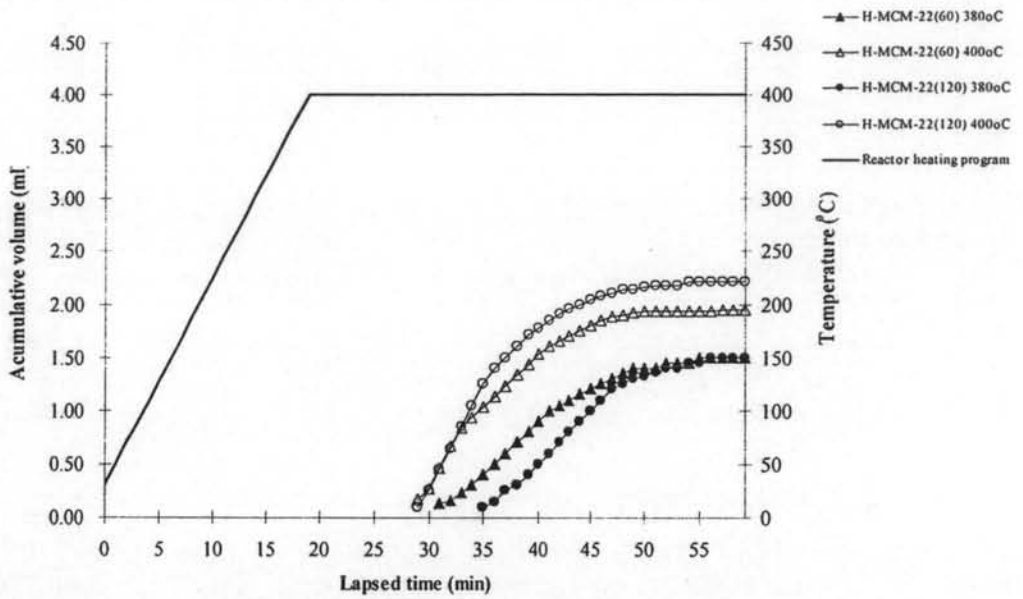

Figure 4.40 Accumulative volume of liquid fractions from HDPE waste cracking over H-MCM-22(60) with two temperatures (Condition: 10%wt catalyst of PP, N_2 flow of 20 cm^3/min and reaction time of 40 min).

Figure 4.41 shows distribution plots of gas fraction obtained by thermal cracking and catalytic cracking of HDPE waste over H-MCM-22 catalysts with two temperatures. In thermal cracking at both temperatures, the distribution in gas fraction is mainly C_5^+. Gas fraction from catalytic cracking over H-MCM-22(60) catalyst at 380°C consists of mainly n-butane, C_5^+ and propene. While the temperature increases, the selectivity to propene increases but that to n-butane decreases. For catalytic cracking over H-MCM-22(120) catalyst, the product distribution in gases phase is slightly different when the temperature increases.

The profiles of gas production distribution are almost not different when changing the SiO_2/Al_2O_3 ratios in the catalyst at both temperatures except the selectivity of n-butane. The gas fraction from the cracking over H-MCM-22(60) at 380°C is rich of n-butane and C_5^+. When the SiO_2/Al_2O_3 ratios increases, the content of n-butane decreases while the selectivity to C_5^+ slightly increase.

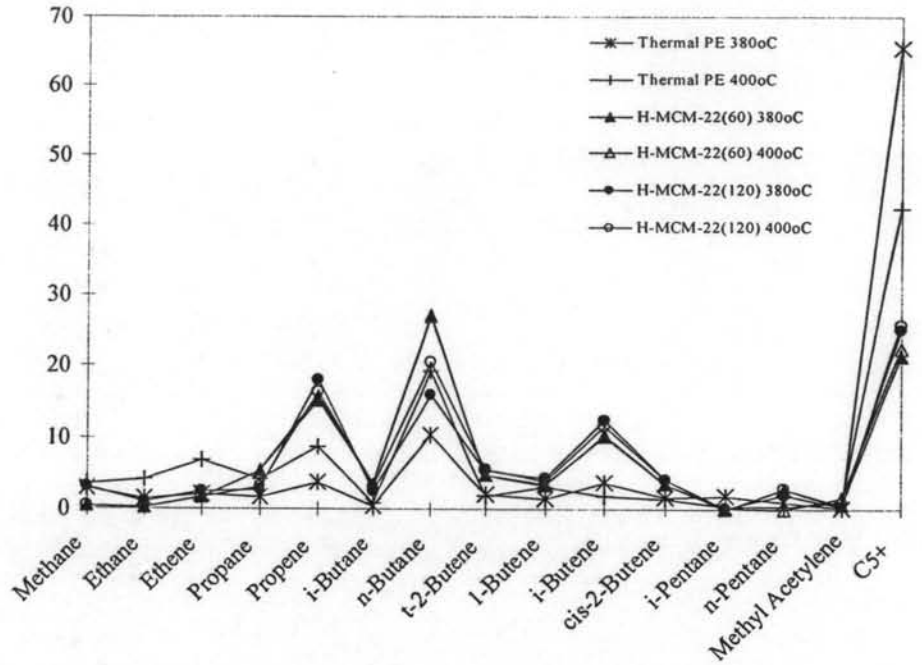

Figure 4.41 Distribution of gas fraction obtained by catalytic cracking of HDPE waste cracking over H-MCM-22(60) with two temperatures (Condition: 10%wt catalyst of PP, N_2 flow of 20 cm^3/min and reaction time of 40 min).

Figure 4.42 shows product distribution of distillated oil obtained by catalytic cracking of HDPE waste over H-MCM-22 catalysts with two reaction temperatures. For HDPE waste cracking over H-MCM-22(60) catalyst at 380°C, the distillated oil components are mainly in range of C_7-C_9. Catalytic cracking at 400°C, the liquid product is mainly C_7 component. When the reaction temperature increases, the liquid fractions of lighter hydrocarbon (C_6-C_7) increases while that of heavier hydrocarbon (C_8-C_9) decreases. Both sample H-MCM-22(60) and H-MCM-22(120) are the same trend.

Catalytic cracking of HDPE waste using H-MCM-22 with SiO_2/Al_2O_3 of 60 at 380°C, the liquid fraction is rich of C_7 and C_8. When SiO_2/Al_2O_3 ratio increases, the component C_8 and C_9 increase. The effect of acidity plays important role on the performance of catalysts with different SiO_2/Al_2O_3 ratios. The results suggest that H-MCM-22 catalysts break the long polymeric chain into small units.

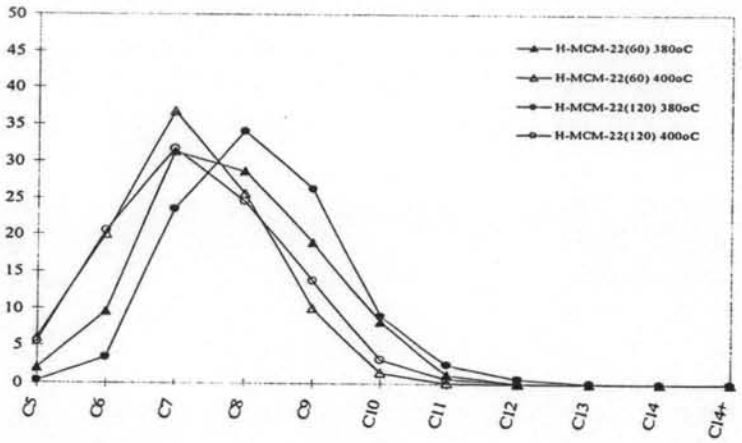

Figure 4.42 Carbon number distributions of liquid fraction obtained by catalytic cracking of HDPE waste cracking over H-MCM-22(60) with two temperatures (Condition: 10%wt catalyst of PP, N_2 flow of 20 cm^3/min and reaction time of 40 min).

4.6 Comparison of catalytic activity in PP waste cracking over H-MCM-22 with other catalysts

Several studies have been described the cracking of polyolefins waste over different acidic solids like zeolites and mesoporous materials. Differences in the catalytic activities of these solids have usually been related to their acid properties. Textural properties, such as surface area and particle size, have been reported to play a key role. For catalytic cracking of PP waste using mesoporous material as catalyst [74], such as Al-SBA-15, promotes PP waste conversion to 97% with 71% of liquid fraction which higher than in case of H-MCM-22, at the same SiO_2/Al_2O_3 ratio. Because it is the effect of large pore size and high total surface area of Al-SBA-15. The distillated oil components are in the range of gasoline for both catalysts. However, liquid fraction mainly consists of heavy oil components in case of Al-SBA-15 while, H-MCM-22 catalyst produces nearly equal amount of light and heavy oil components.

For HDPE waste cracking, Al-MCM-41 (mesoporous material) [75] and H-MCM-22 provide HDPE waste conversion about 94 %. Al-MCM-41 promotes higher liquid fraction yield than H-MCM-22 due to larger pore size and higher specific surface area. Nevertheless, H-MCM-22 catalyst relatively exhibits higher yield of distillate oil than Al-MCM-41, which distillate oil components are mainly in the range of gasoline (C_7-C_8) for both catalysts.